THESIS REPORT

DESIGN & ANALYSIS OF VORTEX TUBE

(EFFECT OF HOT END GEOMETRY ON TEMPERATURE DROP)

SUBMITTED TO

UNIVERSITY OF MUMBAI

FOR THE DEGREE OF

BACHELOR OF ENGINEERING

IN

MECHANICAL ENGINEERING

(2013-2014)

SUBMITTED BY

BHAVESH PARKHE

UNDER THE GUIDANCE OF

DR. PRASANNA NAMBIAR

DEPARTMENT OF MECHANICAL ENGINEERING

DON BOSCO INSTITUTE OF TECHNOLOGY

PREMIER AUTOMOBILES ROAD, VIDYAVIHAR (W)

Design & Analysis of Vortex Tube

(Effect of Hot-End Geometry on Temperature Drop)

Don Bosco Institute Of Technology, Vidyavihar

Project Members

Bhavesh Parkhe (Group No. 31)

Advisor

Dr. Prasanna Nambiar

Project Title : Design & Analysis of Vortex Tube

Group No. : 31

Institute Name : Don Bosco Institute Of Technology

Institute Address : Premier Automobiles Road,
Vidyavihar (W), Mumbai 400070

Project Guide : Dr. Prasanna Nambiar

Project Member : Bhavesh Parkhe (Roll No. 44)

Date of Submission :

Approved By : _____

Dr. Prasanna Nambiar

(Project Advisor)

Department of Mechanical Engineering

Don Bosco Institute Of Technology.

Certificate

This is to certify that Bhavesh Vijay Parkhe, Group No 31, student of BE Mechanical Department, has successfully completed his final year project, Design & Analysis Of Vortex Tube, with the required standards and expectations. This report is a documented proof of the same.

_____ _____

Dr. Prasanna Nambiar **Dr. N. G. Joag**

Advisor & HOD, **Principal**

Mechanical Department

Date :- _____

Acknowledgements

This project wouldn’t have been possible without the kind support of many individuals and organizations. I would like to thank my Project Guide and our Head of the Department, Dr. Prasanna Nambiar, for inculcating the required skills for performing an analysis. I am also thankful to her for generating an interest within students in the field of Computational Fluid Dynamics which is an integral part of my project.

Secondly, I am highly indebted to the workshop faculty and especially Mr. B.S. Patil for their valuable assistance during fabrication of the project.

I would also like to thank and appreciate the help offered by my colleagues Jeet Dabhade, Suraj Hemrajani, Rajiv Warty, Sajil Meledath during various stages of the project.

I am grateful to Don Bosco Institute of Technology for providing us with required assistance and facilities. Lastly, I would like express highest of my gratitude to my parents for their constant support and invaluable help during this project.

The above words are just a fragment of my appreciation towards these people whose contribution in no way I underestimate.

Declaration

I hereby declare that this text is an original compilation of observations in my own language and not a mere verbatim reproduction of sources. There has not been any attempt at replicating any research. There are no manipulations and all the methods used are true to my knowledge. References listed have been properly cited.

Table Of Contents

List Of Figures

List Of Tables

Nomenclature

Symbols	Description
γ	Adiabatic Index
Ac	Cold Exit Area (mm^2)
Ah	Hot Exit Area (mm^2)
Ain	Inlet Area (mm^2)
Avt	Area of vortex tube (mm^2)
Cp	Specific heat at constant pressure (KJ/kg K)
Dc	Cold end diameter (mm)
Dh	Hot End Diameter (mm)
Din	Inlet Diameter (mm)
Dvt	Diameter Of Vortex Tube (mm)
Lvt	Length of Vortex Tube (mm)
mc	Cold Exit mass flow rate (kg/s)
min	Mass flow rate at inlet (kg/s)
pa	Atmospheric pressure (bar)
Pin	Inlet pressure (bar)
Pc	Cold Exit Pressure (bar)
Tc	Cold Exit Temperature (Kelvin)
Th	Hot Exit Temperature (Kelvin)
Tin	Inlet Temperature (Kelvin)

Abstract

The vortex tube is a simple device, having no moving parts, which produces hot and cold air streams simultaneously at its two ends from a source of compressed air. Literature review reveals investigations to understand the heat transfer characteristics in a vortex tube with respect to various parameters like cross section area of cold and hot end, nozzle area of inlet compressed air, cold orifice area, hot end area of the tube, and L/D ratio.

This project presents a comparison between the performance predicted by a computational fluid dynamics (CFD) model and experimental measurements taken using a vortex tube with specifications similar to the commercial one. Also the effect of hot exit geometry is investigated in this report. The protrusion on the hot end blocks major exit portion which raises the back pressure to a certain extent. Attempt has been made validate the experimental results by CFD analysis. The analysis has been done for 3 geometries namely : cone, frustum and flat end. The maximum obstruction diameter is limited to less than that of vortex tube.

Chapter 1: Introduction

The Vortex Tube (VT) cooler is a device that generates cold and hot gas from compressed gas, as shown in Fig. 1. It contains the following parts: one or more inlet nozzles, a vortex chamber, a cold-end orifice, a hot-end control valve and a tube. When high-pressure gas (6 bar) is tangentially injected into the vortex chamber via the inlet nozzles, a swirling flow is created inside the vortex chamber. When the gas swirls to the center of the chamber, it is expanded and cooled. In the vortex chamber, part of the gas swirls to the hot end, and another part exits via the cold exhaust directly. Rest of the gas in the vortex tube reverses for axially and moves from the hot end to the cold end. At the hot exhaust, the gas escapes with a higher temperature, while at the cold exhaust, the gas has a lower temperature compared to the inlet temperature.

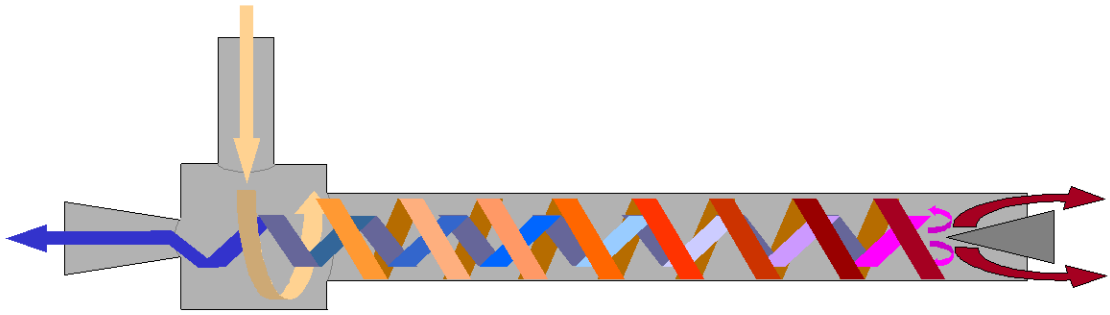

Figure 1: working principle

A Vortex Tube has the following advantages compared to the normal commercial refrigeration device: simple, no moving parts, no electricity or chemicals, small and lightweight, low cost, maintenance free, instant cold air, durable (because of the stainless steel and clean working media), adjustable temperature.

But, its low thermal efficiency is a main limiting factor for its application. Also the noise and availability of compressed gas may limit its application. However, noise can be reduced by using sound mufflers. Vortex tube might be of a better use in applications where compressed air is available readily.

Brief History

The vortex tube was first discovered by Ranque in 1933, and by Hilsch in 1947. In memory of their contribution the VT is also known as Ranque Vortex Tube (RVT), Hilsch Vortex Tube (HVT), and Ranque-Hilsch Vortex Tube (RHVT). The exact theory involved behind this process has not yet been confirmed. There are several theories which have been proposed over the years.

Chapter 2 : Developments over the Years

Since the discovery of vortex tube, there have been many changes in the design as well as theories involving it. In this section, we have tried to discuss the important developments in experimental, theoretical and computational fields. The experimental and theoretical developments listed are as mentioned by C. Gao [9].

Experimental Developments

1) Working Medium

- Mixture of Gases
    i. The first study on the separation of mixtures with the RHVT were published in 1967 by Linderstrom-Lang and in 1977 by Marshall. The gas mixtures (oxygen and nitrogen, carbon dioxide and helium, carbon dioxide and air, and other mixtures) were used as working medium in their work.
    ii. In 2001 the RHVT system was used for carbon-dioxide separation by Kevin
    iii. In 2002 the RHVT system was used to enrich the concentration of methane by Manohar
    iv. In 2004, natural gas was used as working medium and with the RHVT natural gas was liquified by Poshernev
- Steam
    i. In 1979 steam was used as working medium by Takahama.
    ii. In 1979, two-phase propane was used as the working medium by Collins
- Liquid
    i. In 1988 Balmer applied liquid water as the working medium. It was found that when the inlet pressure is high, for instance 20~50 bar, the energy separation effect still exists. So it proves that the energy separation process exists in incompressible vortex flow as well.

2) Geometry

Aspects of the geometry concern the positioning of components like the cold exhaust, control valves and inlet nozzles.

- Direction of flow
  For the positioning of the cold exhaust, there are two different types of RHVT systems proposed by Ranque : counterflow RHVT system and uniflow RHVT system. When the cold exhaust is placed on the other side from the hot exhaust, it is called “counterflow”. When the cold exhaust is placed at the same side of the hot exhaust, it is named “uniflow”.
  From the experimental investigation it was found that the performance of the uniflow system is worse than that of the counterflow system. So, most of the time, the counterflow geometry was chosen. Hilsch was the first to investigate the effect of the geometry on the performance of the RHVT system.

- Placement of control valves and inlet nozzles
    i. In 1955, Westley [24] experimentally optimized the geometry of the RHVT system. He found that the optimum situation can be described by a relationship between the injection area, the tube length, the vortex tube cross sectional area, the cold end orifice area and the inlet pressure
    $$\frac{A_c}{A_{vt}} \simeq 0.167, \frac{A_{in}}{A_{vt}} \simeq 0.156 + 0.176/\tau_p, \text{and } \tau_p = \frac{p_{in}}{p_c} = 7.5$$
    ii. Since the 1960s, Takahama [17, 25–30] published a series of papers on the RHVT. He found that if the Mach number at the exhaust of the inlet nozzle reaches 0.5~1, the geometry should have the following relationship in order to have larger temperature differences or larger refrigeration capacity:
    $$\frac{D_{in}}{D_{vt}} = 0.2, \frac{A_{in}}{A_{vt}} = 0.08 \sim 0.17, \frac{A_c}{A_{in}} = 2.3$$
    iii. In 1969, Soni [10] published a study on the RHVT system considering 170 different tubes and described the optimal performance by utilizing the Evolutionary Operation Technique.
    $$\frac{A_{in}}{A_{vt}} = 0.084 \sim 0.11, \frac{A_c}{A_{vt}} = 0.08 \sim 0.145, \frac{L_{vt}}{D_{vt}} > 45$$

3) Variations in Geometry

- Conical Vortex Tube
    i. In 1961, Paruleker designed a short conical vortex tube. By varying the conical angle of the vortex tube, he found that the parameter Lvt/Dvt can be as small as 3.
    ii. In 1968, Borisenko found that the optimum conical angle for the conical vortex tube should be 3^o
    iii. Takahama introduced the divergent vortex tube (in fact the same as the conical vortex tube but with a different name) in 1981
- Detwisters
  A detwister is some kind of vortex stopper, which can be used to block the vortex motion at the exhausts.
  The detwister was proposed by Grodzovskii in 1954, Merkulov in 1969, and James in 1972. In 1989 Dyskin concluded that the hot-end detwister can improve the performance of the RHVT system and shorten the tube length; the cold-end detwister has the same positive effect on the efficiency
- Double Circuit Vortex Tube
  In 1996, Piralishvili and Polyaev introduced a new type of vortex tube: the Double-Circuit vortex tube with a conical tube to improve the performance. At the hot end, in the center of the control valve, there is an orifice which allows feedback gas to be injected into the vortex tube. The feedback gas has the same temperature as the inlet gas but with low pressure.

4) Internal Flow Field

The investigation of the flow field inside the VT began with flow-visualization techniques such as liquid injection and smoke.

The investigation of the flow field inside the VT began with flow-visualization techniques such as liquid injection and smoke. In 1950 Roy injected colored liquid into the RHVT system to investigate the flow pattern. In 1959, Lay injected water inside the RHVT system, but nothing could be seen. In 1962, Sibulkin used a mixture of powdered carbon and oil. In 1996, Piralishvili used kerosene with the mass ratio of 1:30. In 1962, Smith used smoke.

The visualization techniques can only give us a qualitative description of the flow field inside the vortex tube. For more detailed flow information, like the pressure, temperature, and velocity fields inside the system, probes are required.

Many of researchers used a Pitot tube for pressure measurement and thermocouple to measure the temperature. But intrinsic methods can vary the performance of tube to a certain extent.

Theoretical Developments

1) Adiabatic compression and adiabatic expansion model

The first explanation was given by Ranque. He explained that the energy separation is due to adiabatic expansion in the central region and adiabatic compression in the peripheral region. In 1947 Hilsch used similar ideas to explain the phenomenon in the RHVT, but introduced the internal friction between the peripheral and internal gas layers.

2) Heat transfer theory

In 1951, Scheper proposed a heat transfer theory for the RHVT system based on his experimental work. This model is based on empirical assumptions for the heat transfer and is incomplete.

3) Effect of friction and turbulence

In 1950, Fulton explained that the energy separation is due to the free and forced vortex flow generated inside the system. He stated that: Fresh gas before it has traveled far in the tube, succeeds in forming an almost free vortex in which the angular velocity or rpm is low at the periphery and very high toward the center. But friction between the layers of gas undertakes to reduce all the gas to the same angular velocity, as in a solid body. During the internal friction process between the peripheral and central layers, the outer gas in turn gains more kinetic energy than it loses internal energy and this leads to a higher gas temperature in the periphery

4) Acoustic streaming model

Kurosaka, Chu and Kuroda proposed that the energy separation inside the RHVT is due to the damping of the acoustic streaming along the axis of the tube towards the hot exhaust.

5) Secondary Circulation Model

Ahlborn proposed a so-called secondary circulation model based on his experimental results. He found that the cumulative mass flow over the cross section of the vortex tube in the cold end direction is larger than the cold exhaust flow, which implies the existence of a secondary circulation flow in the VT. With this secondary circulation model, the RHVT can be considered as a classical refrigeration device and the secondary circulation flow can be thought as a classical cycle.

Computational Developments

- Aljuwayhel utilized a fluid dynamics model of the vortex tube to understand the process that drives the temperature separation phenomena.
- Behera used the computational fluid dynamics (CFD) to simulate the flow field and energy separation.
- Skye used a model similar to that of Aljuwayhel. He did a 2D CFD analysis.
- Eisma performed a numerical study to research the flow field and temperature separation phenomenon.
- Kirmaci applied Taguchi method to optimize the number of nozzle of vortex tube.
- Akhesmeh made a CFD model in order to study the variation of velocity, pressure, and temperature inside a vortex tube. Their results obtained upon numerical approach comprehensively emphasized on the mechanism of hot peripheral flow and a reversing cold inner core flow formation.
- Xue Y. discussed on pressure, viscosity, turbulence, temperature, secondary circulation, and acoustic streaming.
- Bramo studied numerically the effect of length to diameter ratio (L/D) and stagnation point occurrence importance in flow patterns.
- Nezhad based on a 3-D CFD model analyzed the mechanism of flow and heat transfer in the vortex tube.

Chapter 3 : Problem Statement

1. The primary objective of the project is to recreate and verify the analysis which is presented in previous papers.
2. This requires recreating an experimental as well as computational model and check whether it conforms to previous analysis.
3. After verifying the claims, the secondary objective is to optimize the performance of vortex tube. In previous attempts of optimization, various geometrical parameters were varied to produce the desired results. Thus, in this analysis, the hot exit geometry will be varied, to study its effects on the performance of the experimental model.
4. Attempt will be made to support the experimental results with a CFD analysis.

Chapter 4 : Experimental Analysis

Description Of Experimental Model

The experimental model was designed taking into account the previous research and empirical relations. Since the definite theory behind the working has not been finalised, most of the data available is experimental data obtained by trial and error methods. Using these previous papers we will finalize the dimensions of our setup.

- Optimum L/D ratio has been found to be 9.3 experimentally as well as numerically. The vortex tube diameter was fixed at 11.5 mm thus fixing the length at 106 mm.
- Inlet Nozzle diameter was fixed upto 3mm for this L/D ratio.
- Number of nozzles – Optimum temperature drop was obtained at 6 nozzles
- Cold end orifice diameter – For the given L/D ratio, the diameter was 6-7mm.
- These dimensions are fairly similar to Exair's 708 slpm vortex tube. Therefor the outer casing dimensions were also kept similar with some additional allowances for fabrication requirements.
- Hot End Orifice Diameter is varied to study the relation of cold mass flow rate vs temperature. A simple nut bolt assembly has been used for that.

Final Dimensions

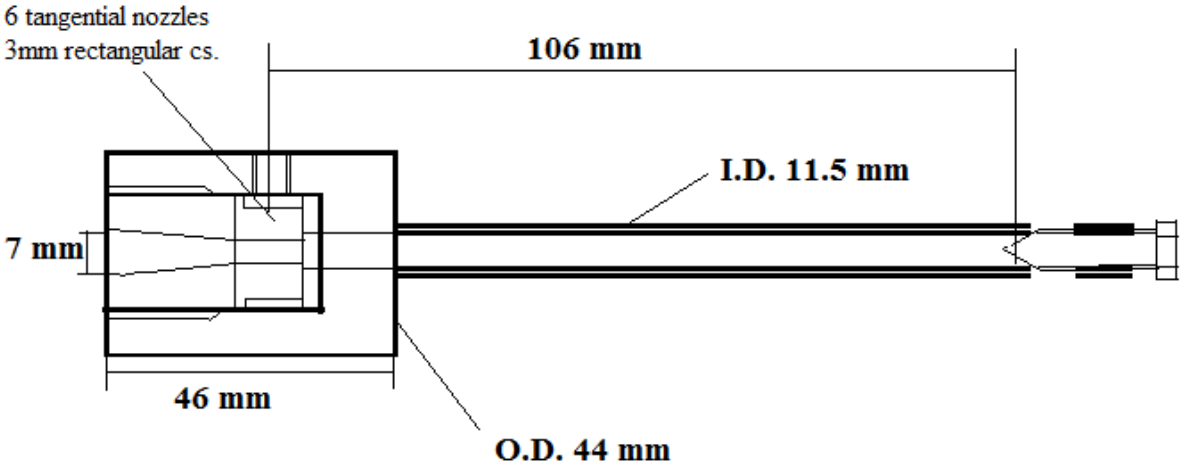

Figure 2 : Dimensions of experimental model

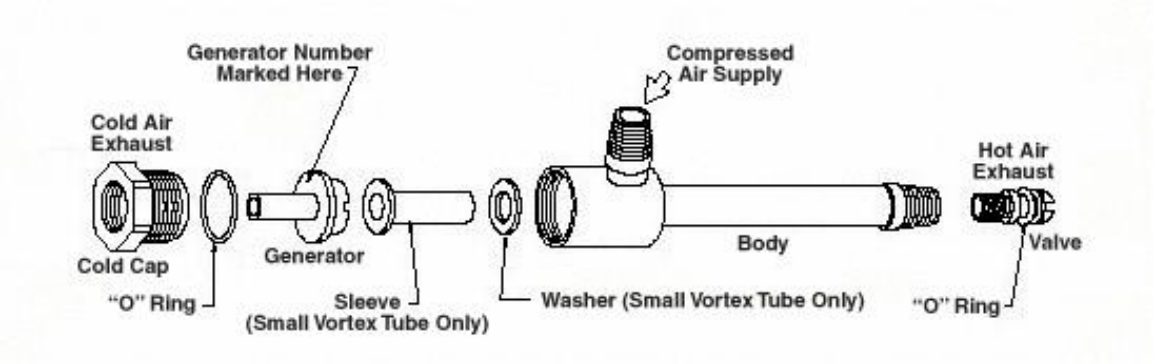

Figure 3 : Exploded view of vortex tube

Experimental Setup

The analysis primarily demands measurement of temperatures and flow rate. Inlet, cold and hot exit temperatures are measured using thermocouples. Inlet and cold exit flow rates are measured in LPM using rotameters. Inlet pressure in measured using pressure gauge and is regulated using a control valve.

Figure shows the schematic of the experimental setup. The detail of each equipment is given below.

- Pressure Regulator – Ball Type Valve
- Pressure Gauge – Range 0-7 bar (upto 100psi)
- Rotameter – Range 0 to 500 LPM Air.
- Thermocouple Junction – J type

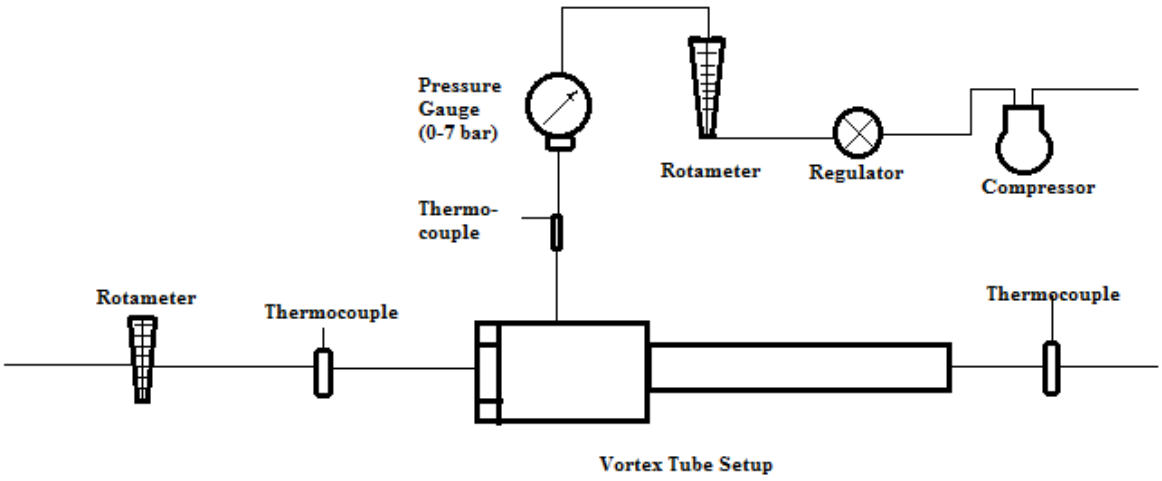

Figure 4 : schematic diagram of experimental setup

For measuring the temperature gradients and velocity variations at different points in the vortex tube, intrinsic methods have to be used. Thus several holes are drilled at different lengths from the inlet as shown in figure. Angle of the flow is measured clockwise from negative X axis.

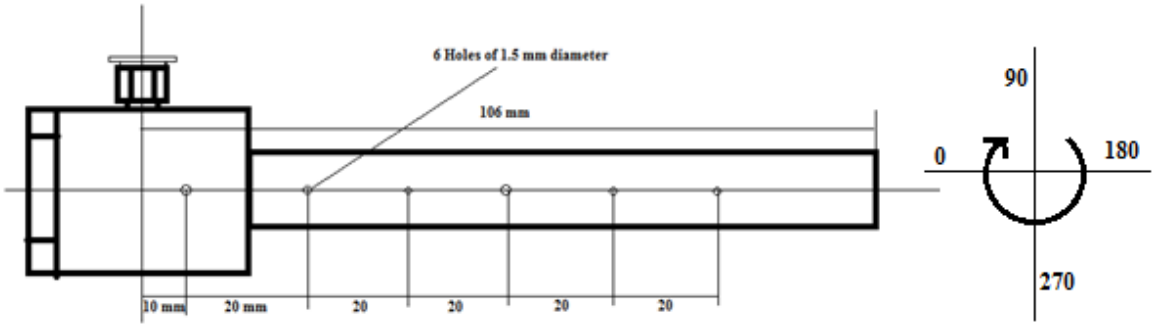

Figure 5 : Placement of holes with respect to inlet

These holes are used for two reasons –

1. For measurement of temperature gradients using thermocouple junction.

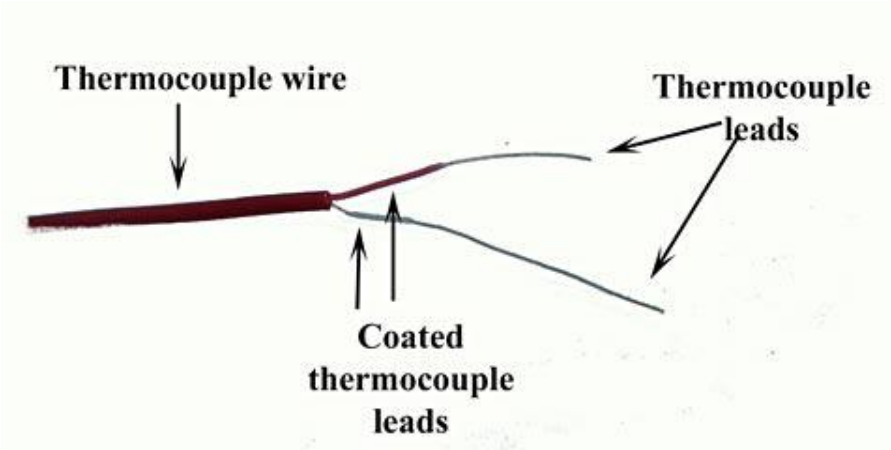

Figure 6 : Thermocouple

/

2. For measuring the static and dynamic pressure and thereby determine the flow characteristics at various diameters.
    - For this purpose the pitot tube principle is being employed.
    - A thin brass tube of 1.5 mm outer dia. With a hole at side of diameter 0.5 mm is being used as a pitot tube.
    - This type of tube has been calibrated by Chengming Gao and is thus suitable to use in this case.
    - A pressure gauge of range 0-2 bar has been used to directly indicate static pressure.
    - The tube is attached to the gauge by the means of appropriate adapters and is checked for leaks before usage.

- The pitot tube arrangement is as shown in fig.

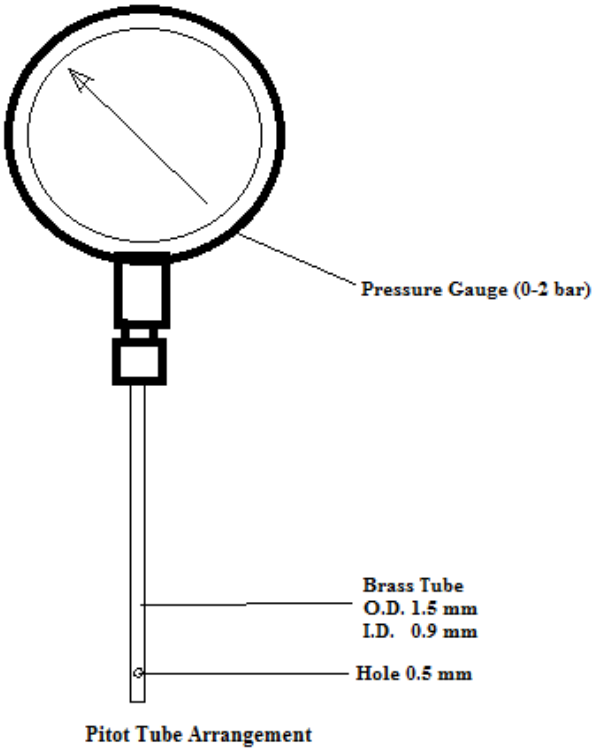

Figure 7 : Pitot tube arrangement

Geometry of Hot End

This research was also done to find the effect of hot end orifice geometry on the performance of the vortex tube. Performance parameters which were measure mainly were temperature drop and flow rate. Following were the geometries for which the testing was done. A simple nut-bolt arrangement was used to vary the area.

1. Cone Geometry
   The orifice diameter can be varied with the help of a cone arrangement. The max orifice diameter was fixed to 11.4 mm.

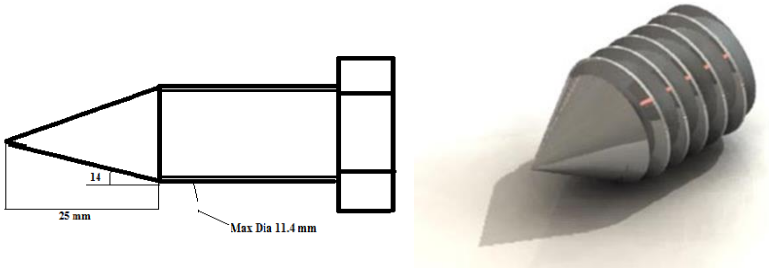

Figure 8 : Cone Dimensions

2. Frustum Geometry
   Convergence angle same as for cone geometry (14^{O}). Maximum diameter also similar (11.4mm) to cone.

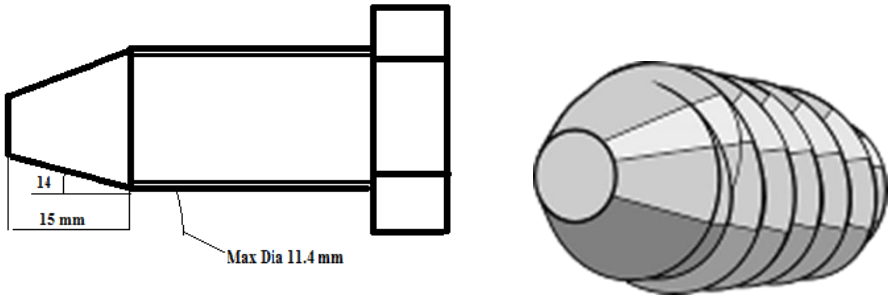

Figure 9 : Frustum Dimensions

3. Flat geometry
   Maximum diameter - 11.4 mm.

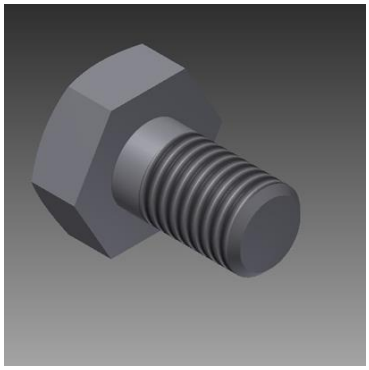

Figure 10 : Flat End

The different geometries proposed are a protrusion on a bolt of 11.4 mm diameter. The distance measured in this analysis is from the initial maximum diameter point. For eg. for cone the base has the max diameter, thus, the istace is measured with respect to the base. The base is marked as zero and point beyond and ahead of that are marked as positive and negative respectively.

Observations - Effect Of Hot End Geometry

In this analysis, the flow rate and temperature are measured with respect to the cold exit opening. The length of the opening is measured from the point of maximum diameter, which is at the base in case of cone & frustum, to the cold exit. The maximum diameter is taken as point zero and the position is measured with respect to this point.

Observation Tables

1. **Cone End**

Table 1 : Inlet Pressure – 6.2 bar

Length	-1.2	-0.9	0	0.3	0.6	0.9	1.8	2.1	3.1	4
Temperature	283	273	253	258	261	263	268	269	271	273
Flow Rate	27	30	51	63	78	85	100	109	117	125

Table 2 : Inlet pressure - 4 bar

Length	-0.5	-0.4	0	0.15	0.5	0.9	2.2	3.1
Temperature	273	267	262	263	265	268	273	274
Flow Rate	28	29	39	47	50	67	84	92

2. **Frustum End**

Table 3 : Inlet Pressure – 6.2 bar

Length	-1	-0.6	-0.45	-0.25	0	0.1	0.2	0.3	0.6	0.9	1	1.2	1.7
Temperature	283	278	273	260	253	258	260	263	265	267	269	271	273
Flow rate	30	38	42	48	56	67	73	76	85	100	110	112	130

Table 4 : Inlet Pressure – 4 bar

Length	-0.8	-0.5	-0.4	-0.1	0.1	0.3	0.5	0.9	1.1
Temperature	278	273	268	262	265	267	269	271	273
Flow Rate	24	30	32	41	48	52	65	72	87

3. **Flat End**

Table 5 : Inlet Pressure – 6.2 bar

Length	-1.4	-1	-0.9	-0.85	-0.8	-0.6	-0.5	-0.4	-0.2	0.1	0.3	0.4	0.5	1	1.7	2	2.3	3.1	3.5	4	4.7	5.3
Temperature	290	280	273	267	263	258	253	255	256.5	258	259	260	261	262	264	265	266	267	268	269	270	271
Flow Rate	4	23	25	28	34	37	46	52	58	65	69	75	83	90	102	105	107	115	120	125	130	131

Table 6 : Inlet Pressure – 4 bar

Length	-0.4	-0.35	-0.3	0.1	0.2	0.8	1	1.2	1.5	2.3	3.1
Temperature	283	273	268	262	263	264	265	266	268	271	273
Flow rate	25	26	27	37	45	52	56	60	67	78	80

Observations – Graphical Representation

1) Flat End

Inlet Pressure - 6.2 bar

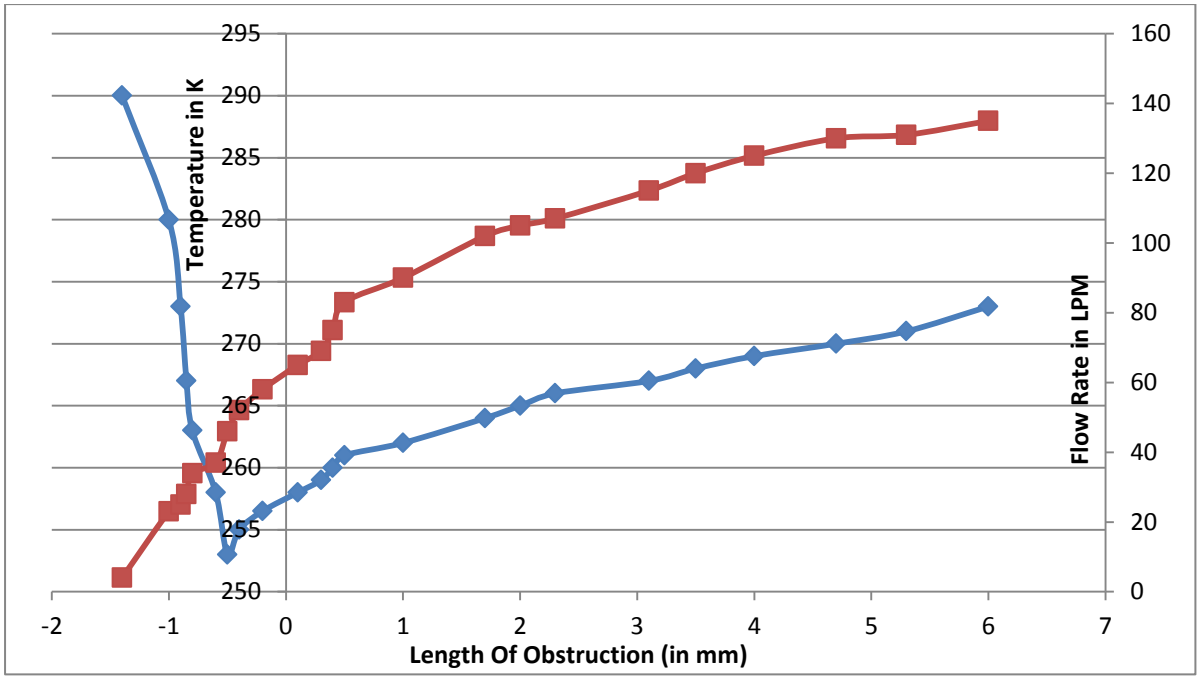

Figure 11 : Length vs Temperature (blue), Length vs Flow Rate (Red)

Inlet Pressure - 4 bar

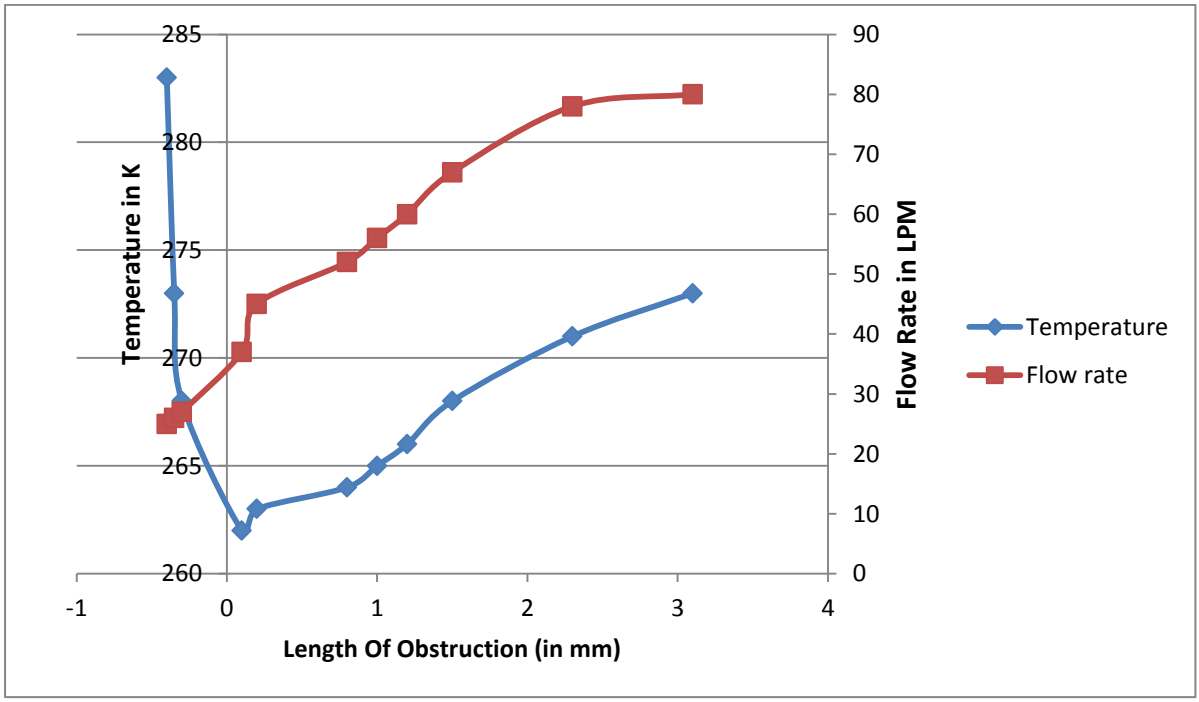

Figure 12 : Length vs Temperature (blue), Length vs Flow Rate (Red)

2) Frustum End

Inlet pressure - 6.2 bar

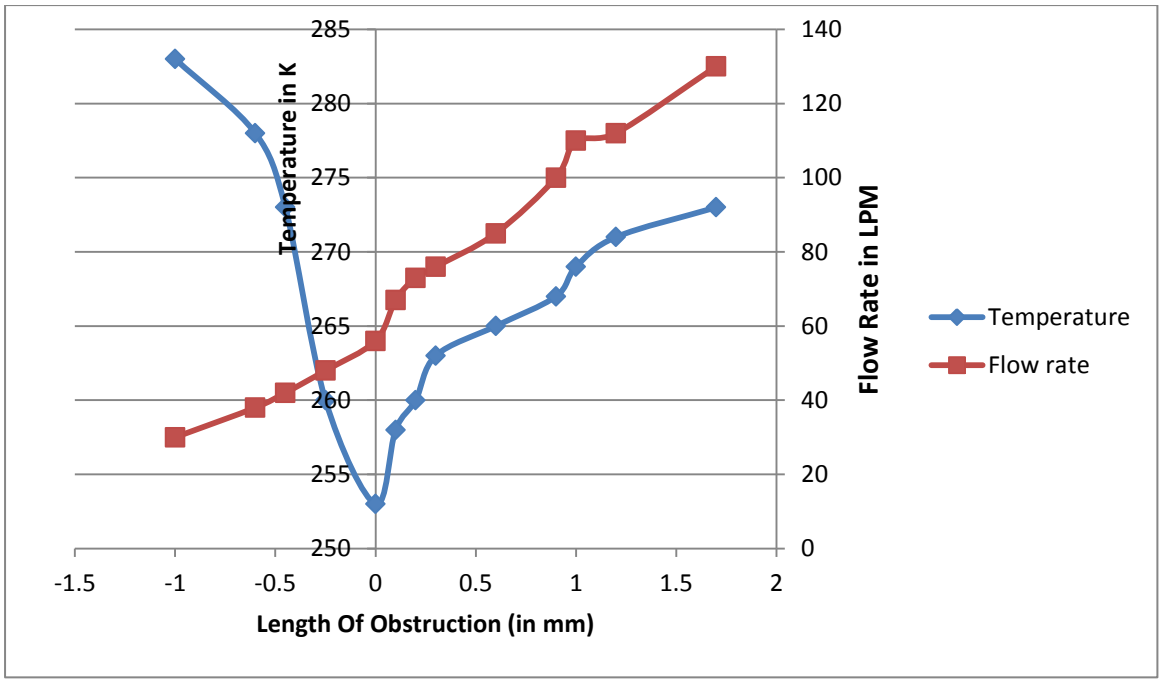

Figure 13 : Length vs Temperature (blue), Length vs Flow Rate (Red)

Inlet Pressure - 4 bar

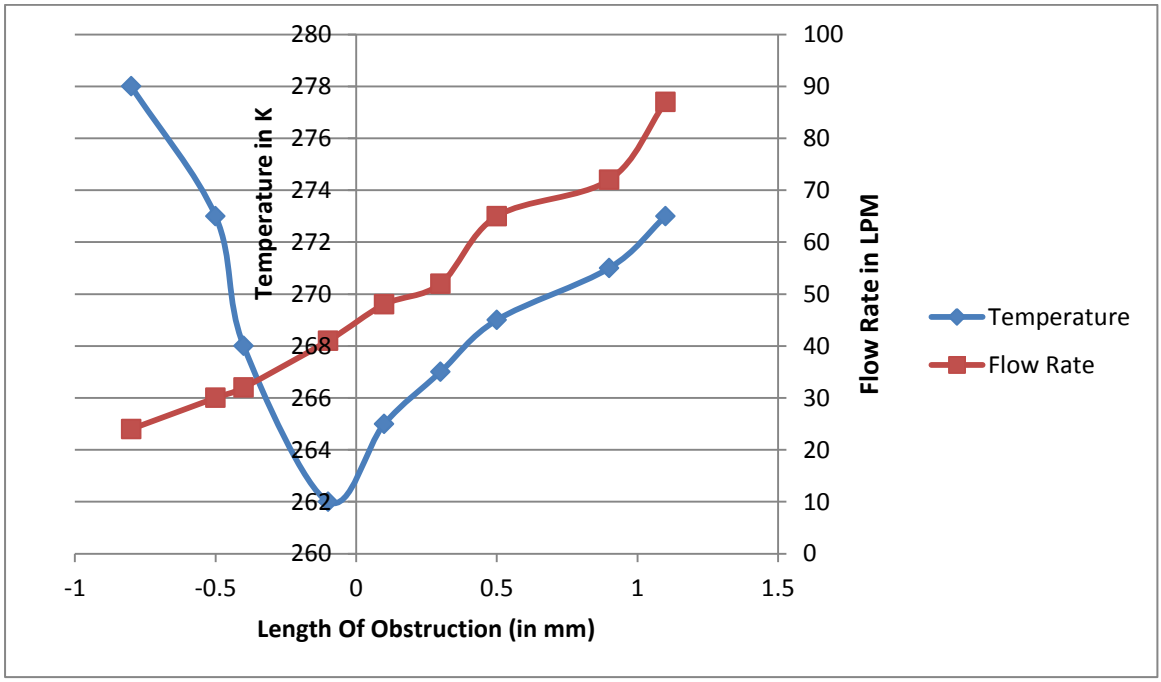

Figure 14 : Length vs Temperature (blue), Length vs Flow Rate (Red)

3) Cone End

Inlet Pressure 6.2 bar

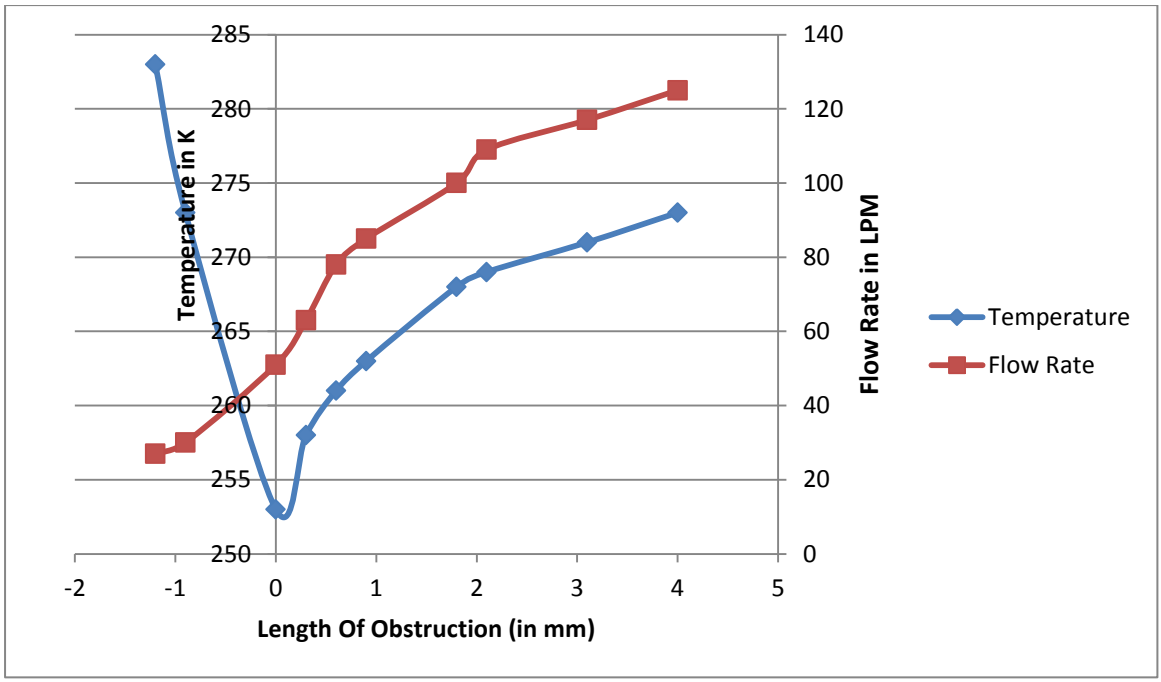

Figure 15 : Length vs Temperature (blue), Length vs Flow Rate (Red)

Inlet Pressure 4 bar

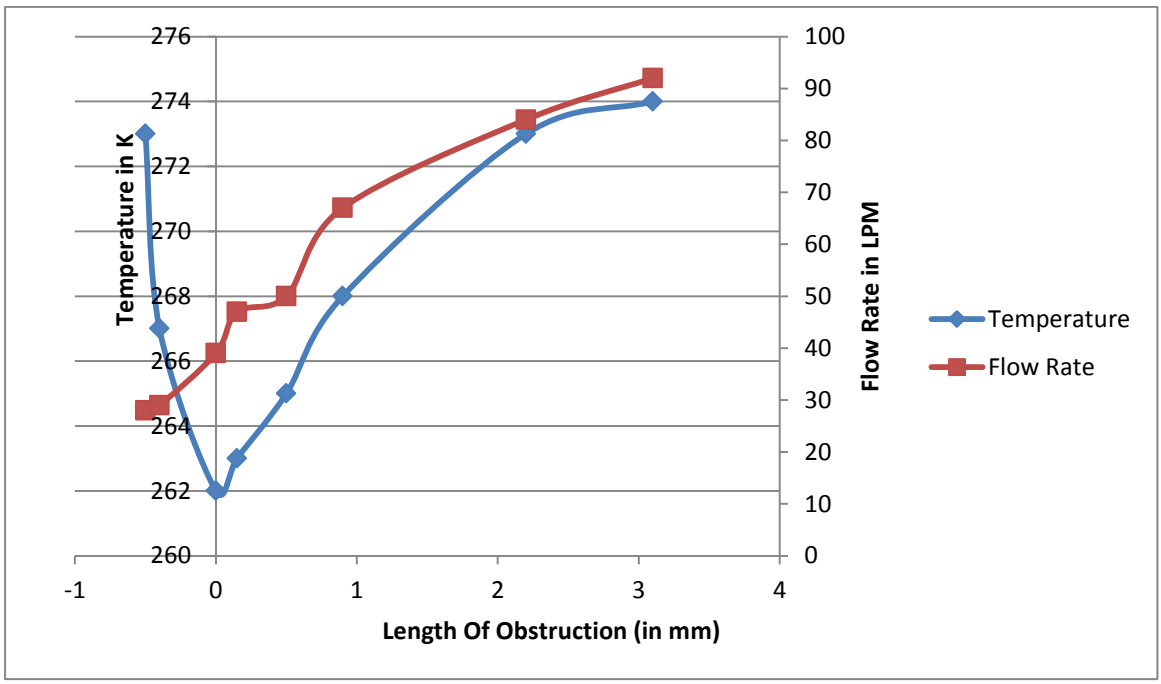

Figure 16 : Length vs Temperature (blue), Length vs Flow Rate (Red)

Comparison between flow rates (pressure 6.2 bar)

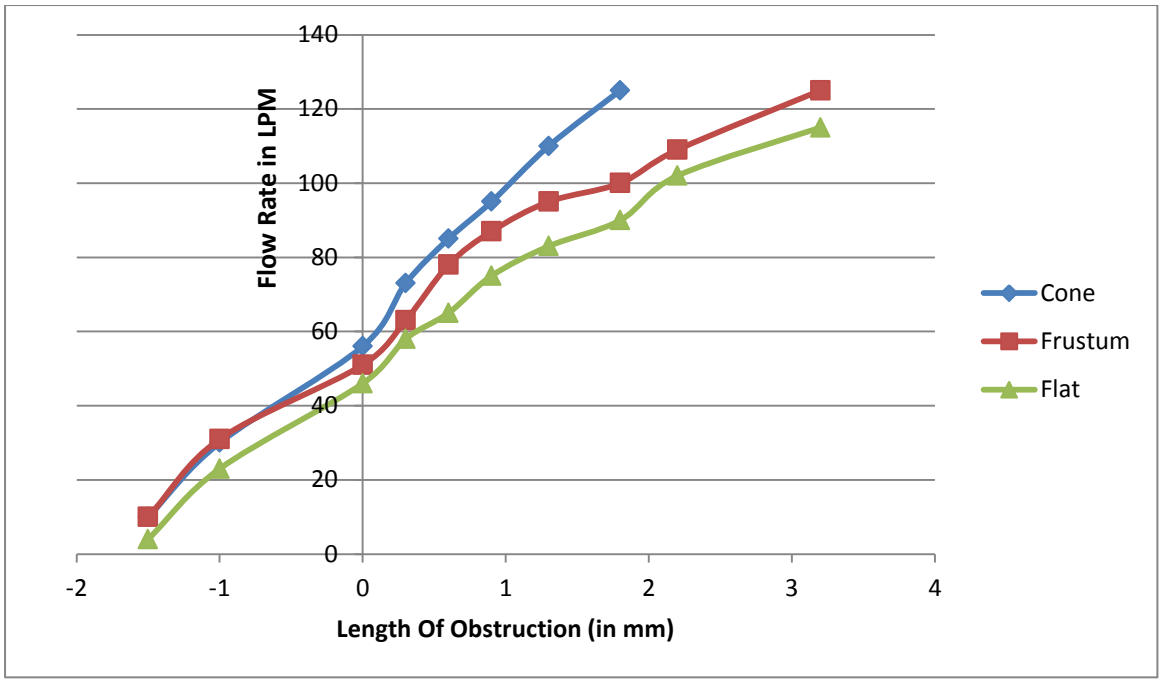

Figure 17 : Comparison between flow rates (Length vs flow rate)

Comparison of Temperatures (pressure 6.2 bar)

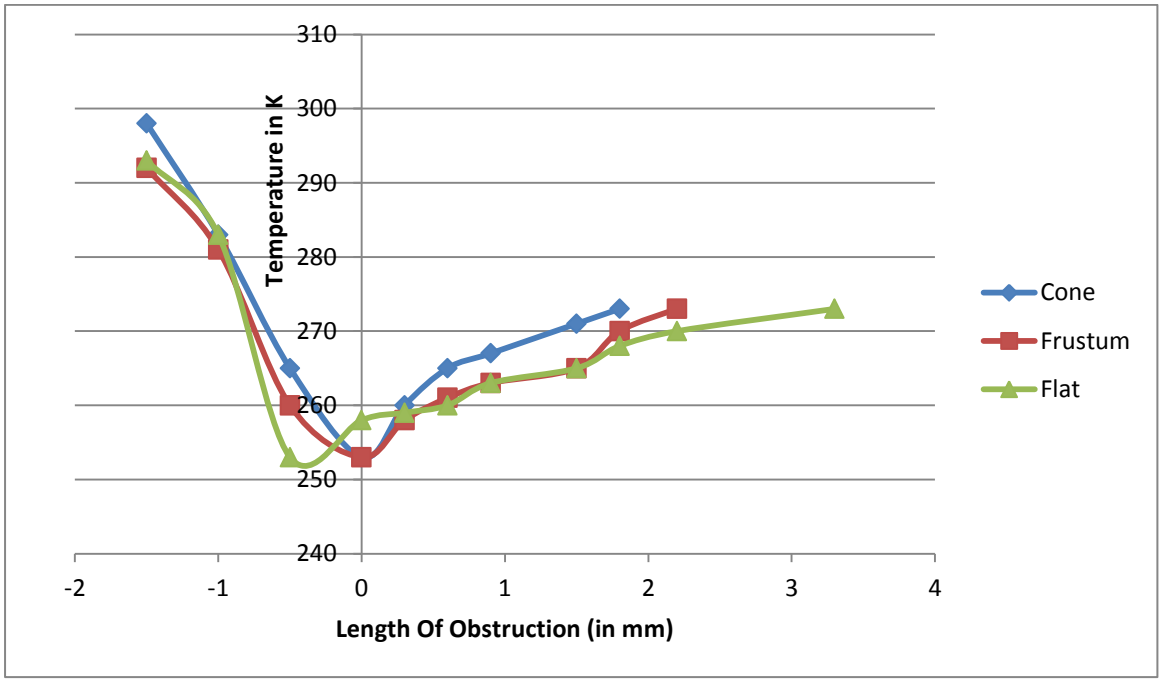

Figure 18 : Comparison of temperatures (Length vs temperatures)

Comparison between flow rates (pressure 4 bar)

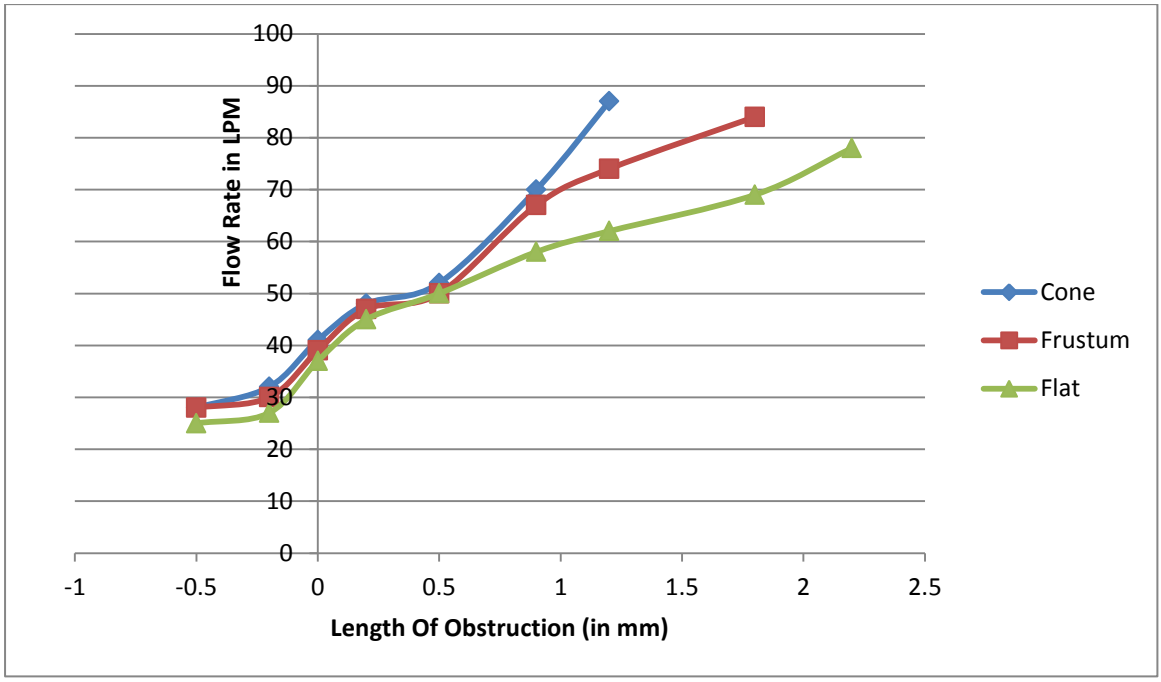

Figure 19 : Comparison between flow rates (Length vs Flow Rate)

Comparison between temperatures (pressure 4 bar)

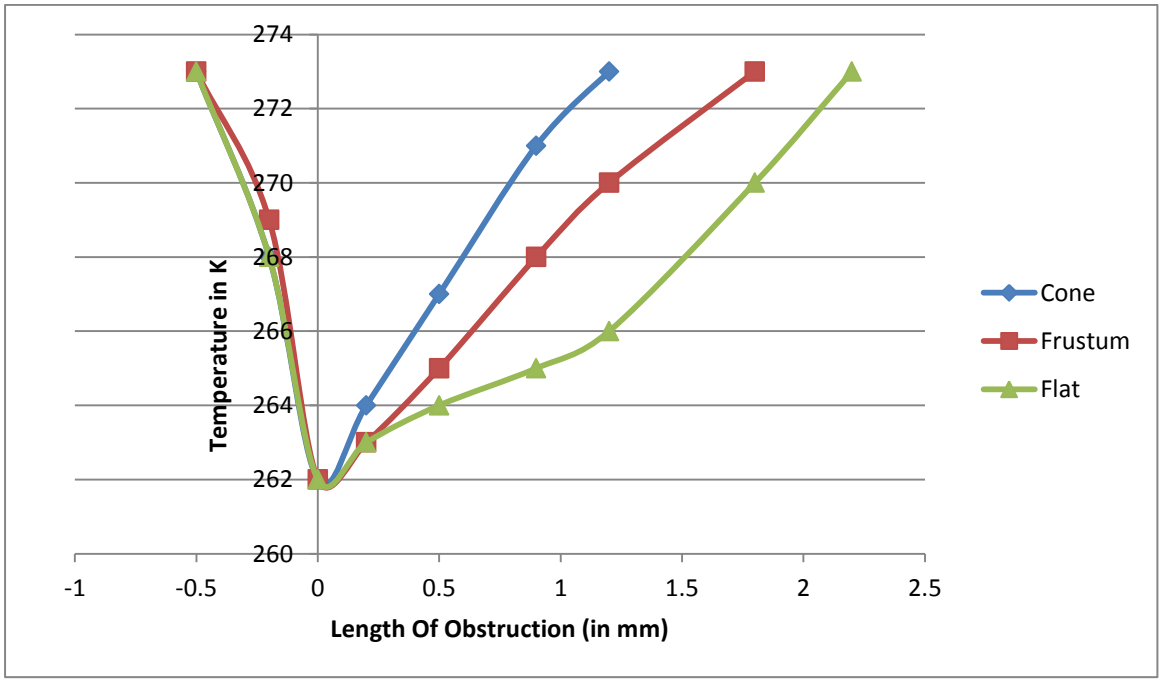

Figure 20 : Comparison between Temperatures (Length vs Temperature)

Comparison with documented experimental results

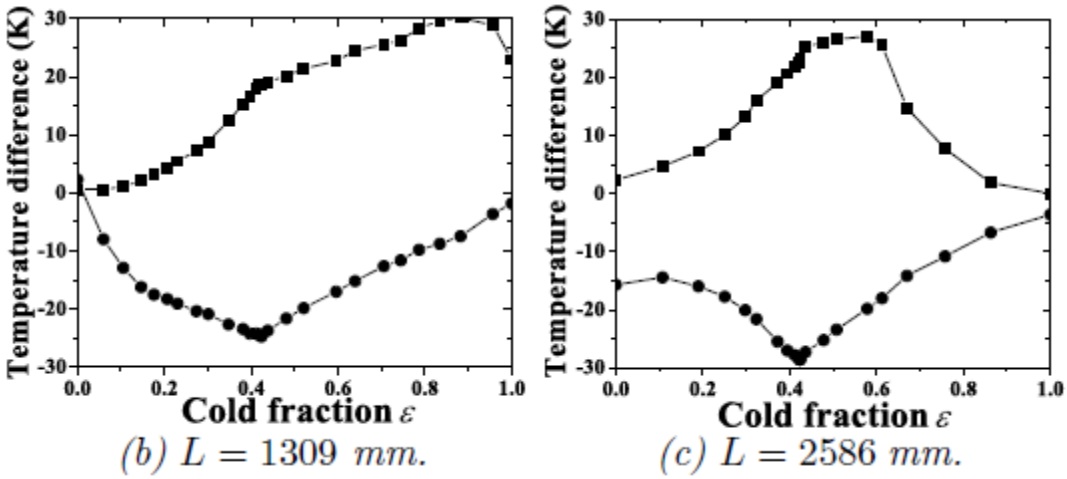

Figure 21 : Cold Temperature Difference vs Cold fraction

The above figure shows cold temperature against cold fraction whereas the lower one shows against the length of the obstruction. The length and cold fraction are proportional as shown by the red plot. The pattern of temperature drop is similar to the observations made in other papers. Comparison is based on the well-established assumption that length of obstruction is proportional to cold fraction.

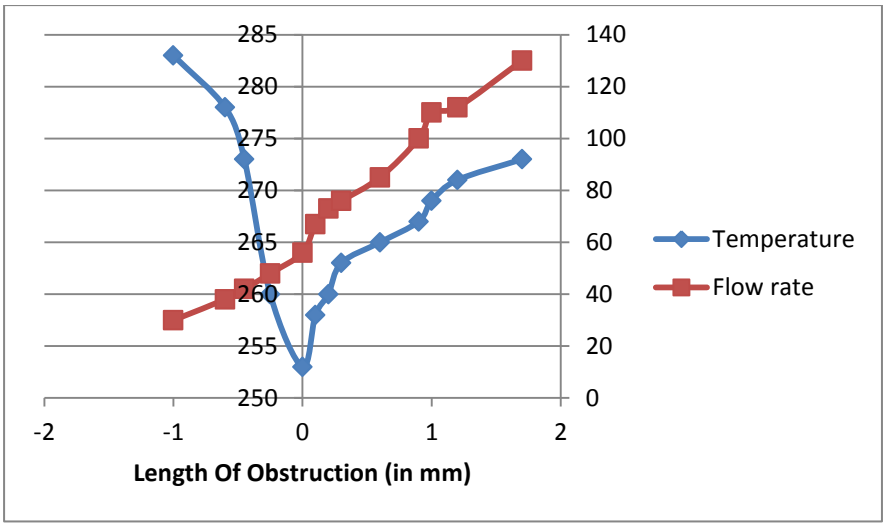

Figure 22 : Length vs Cold End Temperature

Results

1. **General**

- The minimum temperature first decreases and then goes on increasing with increase in the length of obstruction.
- The flow rate increases with increase in length.
- The temperature drop reduces considerably with change in pressure (For 6.2 bar 253 K, for 4 bar 262 K)

2. **Comparison between different geometries**

- The temperature profile of all three geometries is almost similar. The minimum temperature is achieved earlier by flat geometry as compared to other two.
- The flow rate goes on increasing as we go from flat, frustum to cone.
- The improvements in flow rate are minor at lower temperatures and go on increasing with increase in temperatures.

Conclusion

The hot end geometry does not affect the minimum temperature produced b the vortex tube. However it does affect the flow rate. Cone shaped protrusion gave the maximum flow rates compared to frustum and flat end.

Chapter 5 : CFD Analysis

Computational Fluid Dynamics plays an important role in determining the performance of projects in a simulated environment. CFD has emerged as one of the essential and necessary tools for any analysis. Therefore, analysing the working of vortex tube using appropriate CFD software and comparing it to experimental observations.

Description

ANSYS Fluent 14.5 was used to create simulation of the given model. The analysis was done for all three geometries (cone, frustum, flat). Previous attempts of analysis have been taken into consideration for current analysis.

Geometry

The CFD model was similar to experimental model of vortex tube in terms of dimensions. The model was simplified to focus on behaviour of air after exiting the tangential nozzle. CFD analysis was done for all three hot end geometries namely – cone, frustum and flat.

Mesh

Unstructured Mesh with finer grids near inlet and both the outlets was used. Meshing was done using ICEM CFD to facilitate periodic linking. Part structured meshing was used for some parts.

Fluent Analysis

The analysis was done for a steady state condition, with a density based solver. Turbulence was predicted and on the basis of previous papers, k-epsilon model was selected. The constant values (Cmu, C1, C2, TKE etc.) were set to default. Energy equations were applied and viscous heating was selected.

Boundary Conditions

- Inlet (mass flow inlet)
  Total Mass flow rate – 0.00826 kg/s. Static Temperature 298 K
- Cold Outlet was set as a pressure outlet with ambient pressure condition.
- Hot Outlet the pressure was set as 0.56 bar gauge owing to the back pressure.

Results and Discussions

Temperature gradients are similar to previous observations. Minimum outlet temperatures are almost similar for all three geometries as in the case of the experimental model. Also the velocity gradients correspond to experimental observations.

Mesh & Geometry

1. Cone End

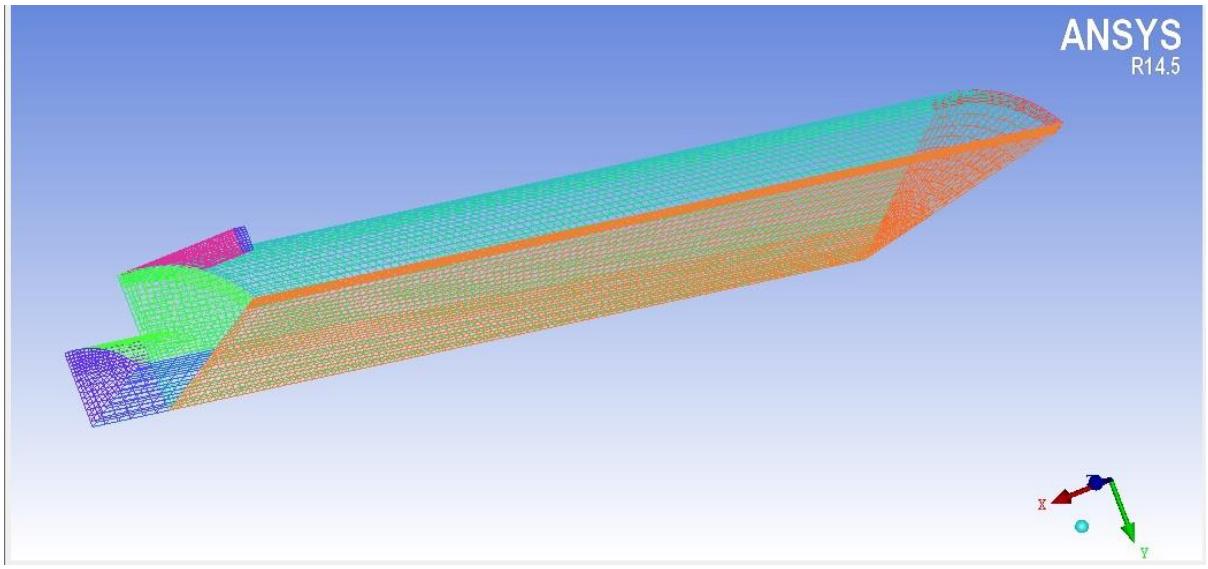

Figure 23 : ICEM Mesh for cone end geometry

2. Frustum Mesh

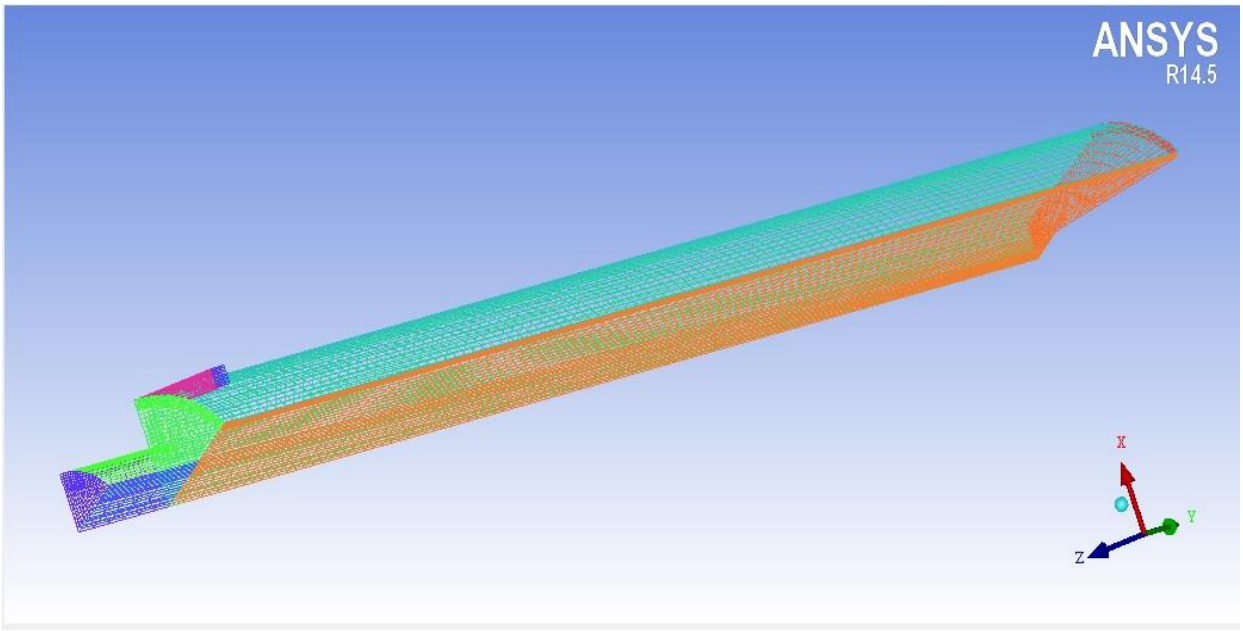

Figure 24 : ICEM Mesh for Frustum end geometry

3. Flat End

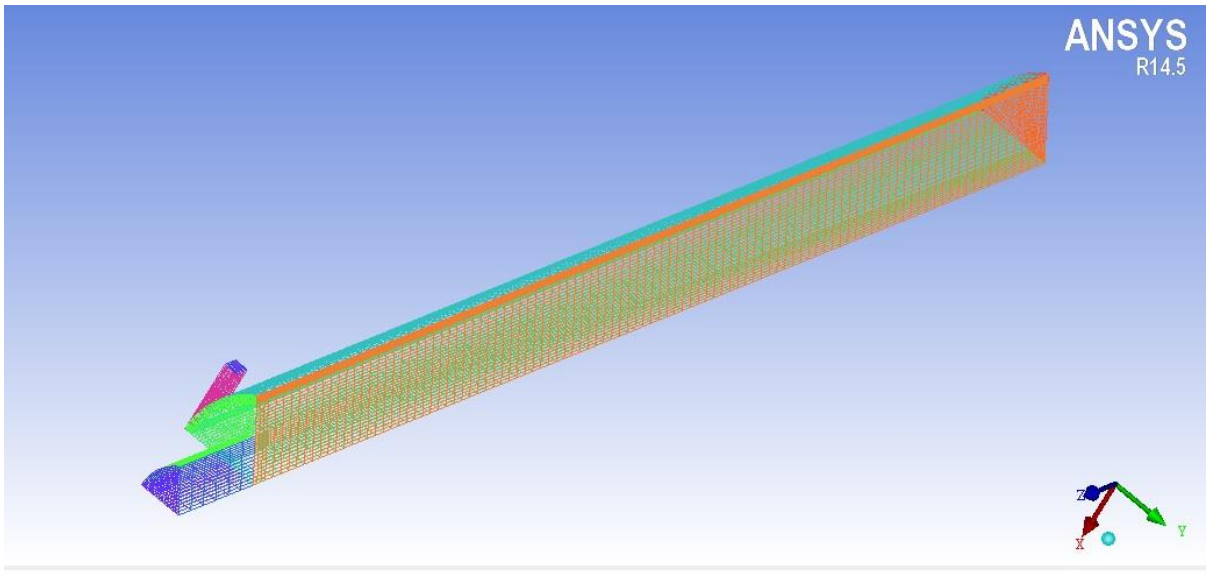

Figure 25 : ICEM Mesh for Flat end geometry

Temperature Gradients

1. Cone

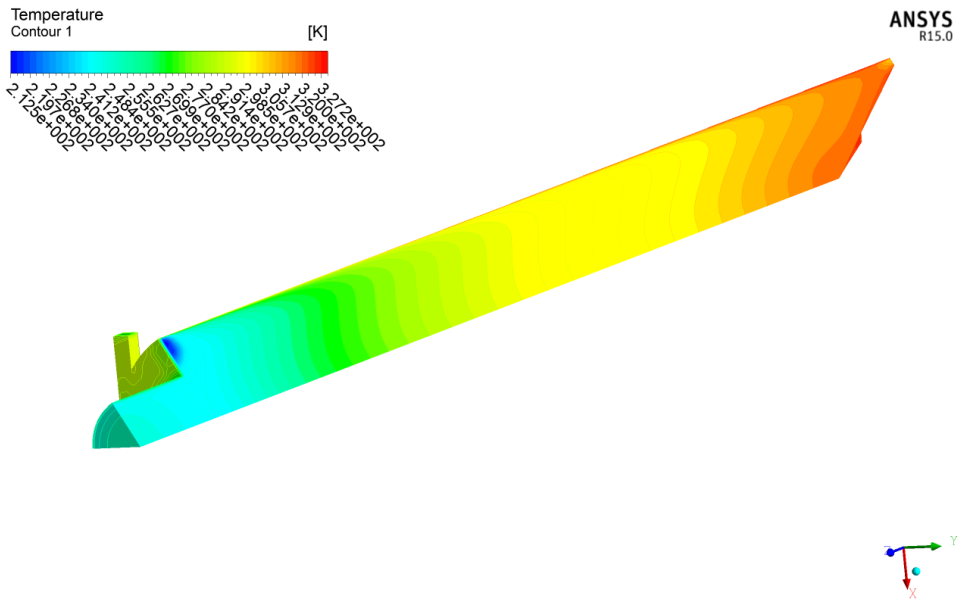

Figure 26 : Temperature Contours for Cone End

2. Frustum

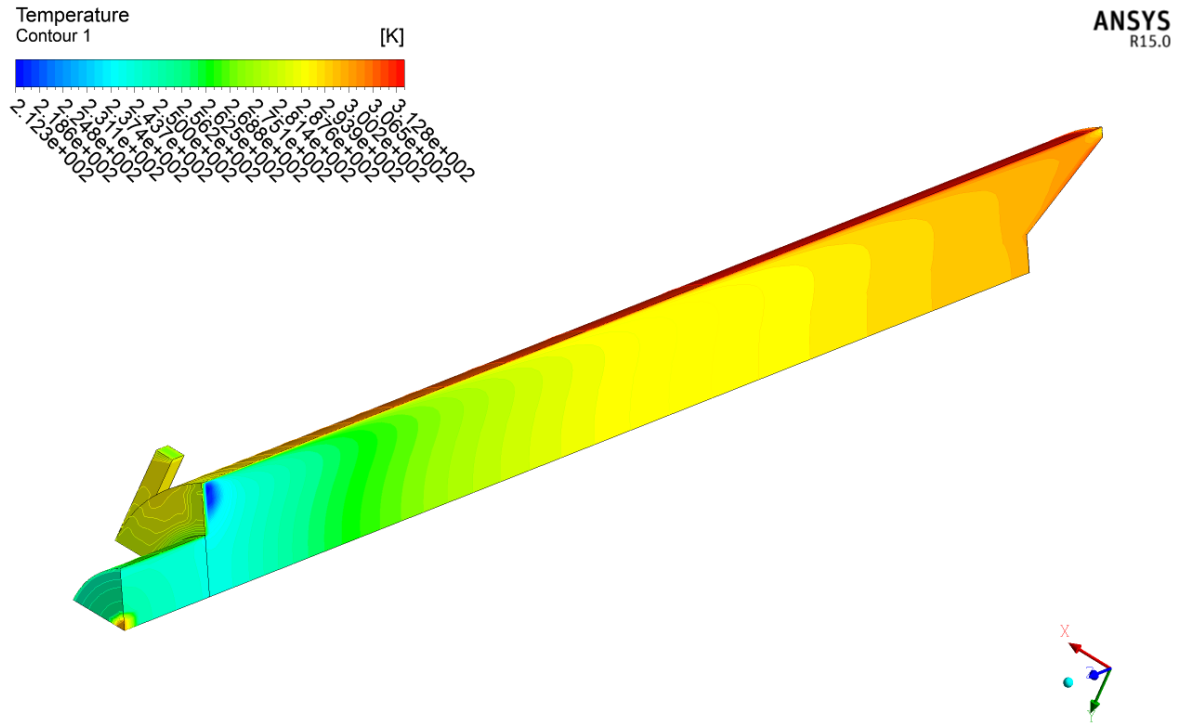

Figure 27 : Temperature Contours for Frustum End

3. Flat

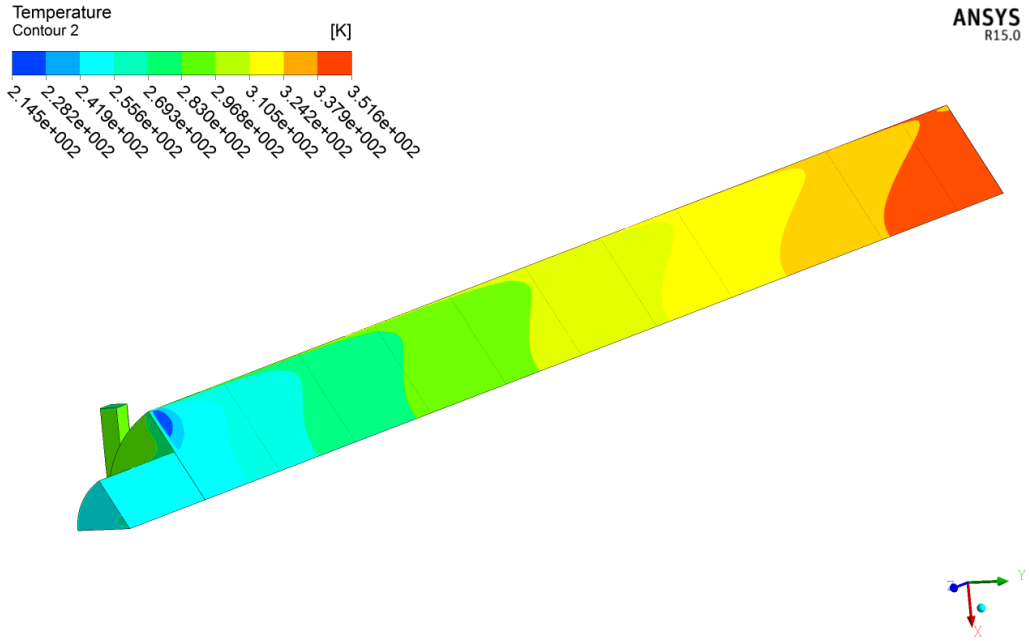

Figure 28 : Temperature Contours for Flat End

Temperature Vectors (Cone)

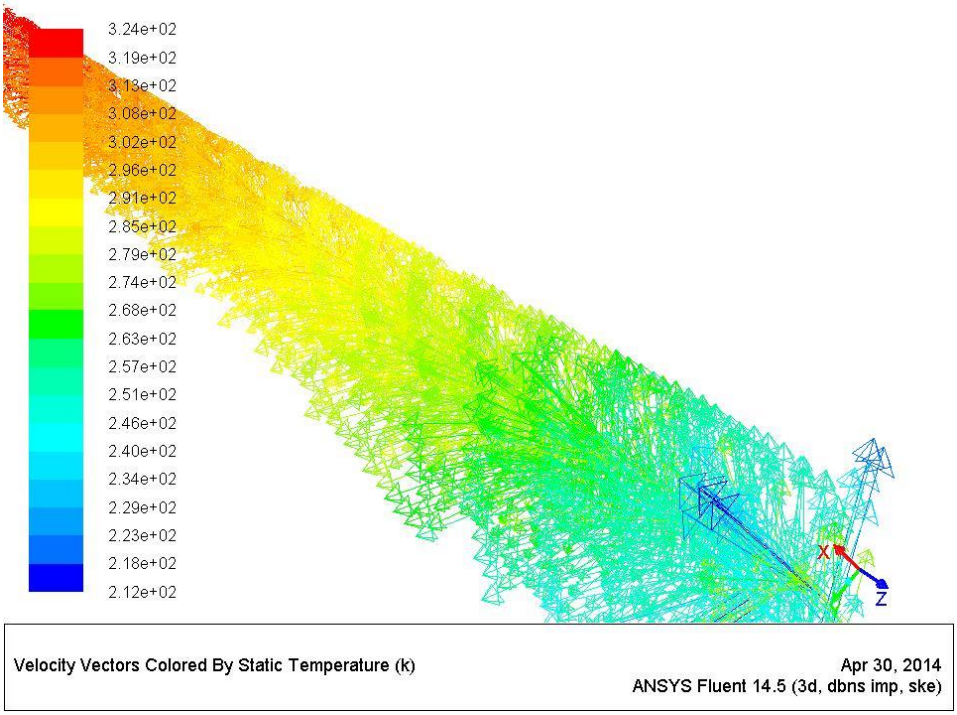

Figure 29: Temperature Vectors for Cone

This fig. shows the direction of rotation of the vortex.

Comparison with Previous Documented Results

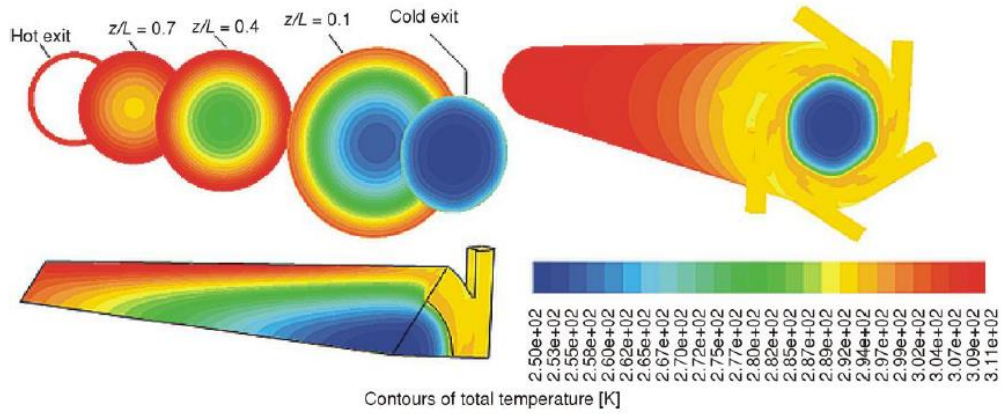

Figure 14. Contours of total temperature at z/L = 0.1, z/L = 0.4, z/L = 0.7.

Figure 30 : Temperature Contours- CFD analysis by A. Bramo & N. Pormahmoud

The results of CFD analysis were similar to that of previous papers. The temperature gradients observed are similar. Minimum temperature of 253 K which is obtained in this analysis is approximately close to 253 K observed by Bramo & Pormahmoud [4].

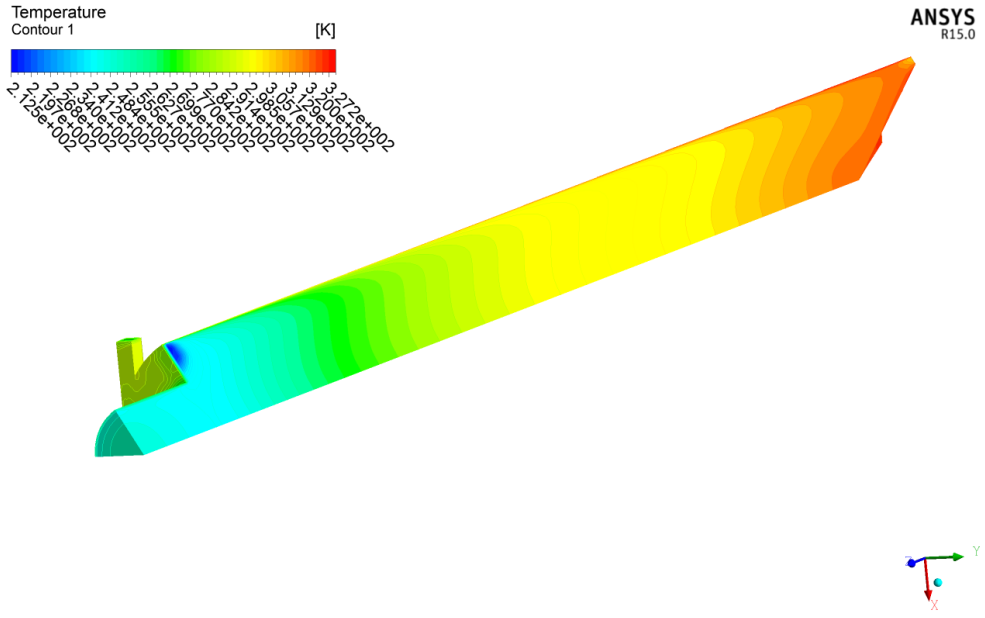

Figure 31 : Temperature Contours for Experimental Model

Exceptions

The boundary conditions stated were same for all three geometries. However, the mass flow rate differences did not conform with the experimental results. This was because the minimum temperature in flat geometry was not achieved at complete blockage of hot exit. Obstruction was a bit farther (as indicated in the graph). Thus, back pressure will be lower. Hence a different boundary condition for hot outlet pressure was given (0.4 bar).

Results

The minimum temperature obtained remained similar for the three models . The temperature gradients and the velocity vectors match the experimental data upto certain extent.

After accounting for the above exception, the difference in flow rates was observed. The mass flow rate through cold exit was maximum for the cone end.

Conclusion

1. CFD analysis can be used to determine the performance of the vortex tube under various conditions.
2. To obtain significant changes in the mass flow rate, the back pressure on the hot exit needs to be varied depending on the experimental conditions.

.

Comparison between CFD and Experimental model

Experimental	Computational	Comments
Minimum temperature at cold exit 253 – 252 K	Minimum temperature at cold exit 250 – 253 K	Minimum temperatures conform owing to the given boundary conditions
Flow vectors Vortices are formed in the CCW direction as view from cold side.	Flow vectors Vortices are formed in direction of nozzle	
Vortex Velocities High velocities at the periphery which gradually decrease towards the center	Vortex velocities High velocities at periphery with a reverse flow near the cold exit.	
Hot Exit Maximum temperatures 323 – 325 K	Hot Exit Temperatures 325 – 330 K	Approximately similar
Cold Mass Flow Rate • Cone – 0.0013 kg/s • Frustum – 0.0011 kg/s • Flat – 0.00102 kg/s	Cold Mass Flow Rate • Cone – 0.003 kg/s • Frustum – 0.0027 kg/s • Flat – 0.0022 kg/s	Mass flow rate was lesser than predicted because of leakages owing to intrusive measurement techniques

Table 7 : Comparison Between CFD and Experimental model

Chapter 6 : Velocity Gradients (Dynamic pressure gradients)

The dynamic pressure readings cannot be used to calculate the velocity accurately because of intrusive measurement techniques. Calibration of the pitot tube arrangement was not done separately. Therefore, the dynamic pressure readings will be only used to observe flow direction and their intensity.

The hole of pitot tube is rotated by 360^{o} inside the flow field at different radii. The angle is measured clockwise from the negative X axis direction as shown in fig. 5.

- **Pressure 6 bar (Pressure vs Angle)**
  - Hole 1 (10 mm from inlet)

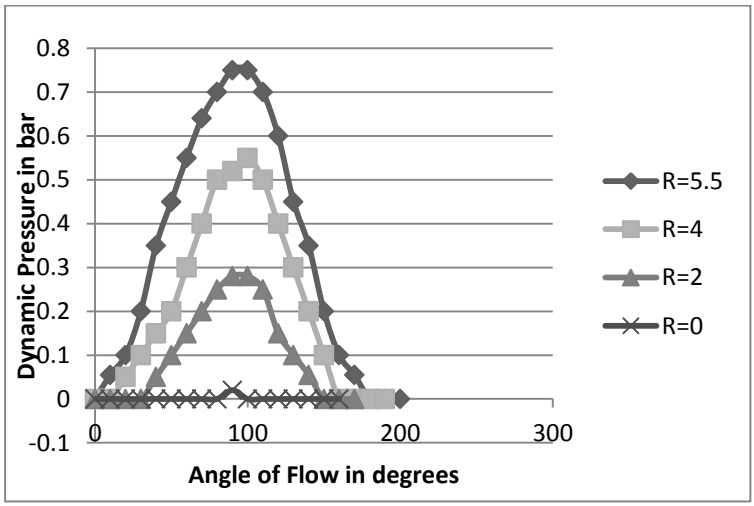

Figure 32 : Dynamic Pressure vs Angle of Flow for Hole 1

  - Hole 2 (30 mm from inlet)

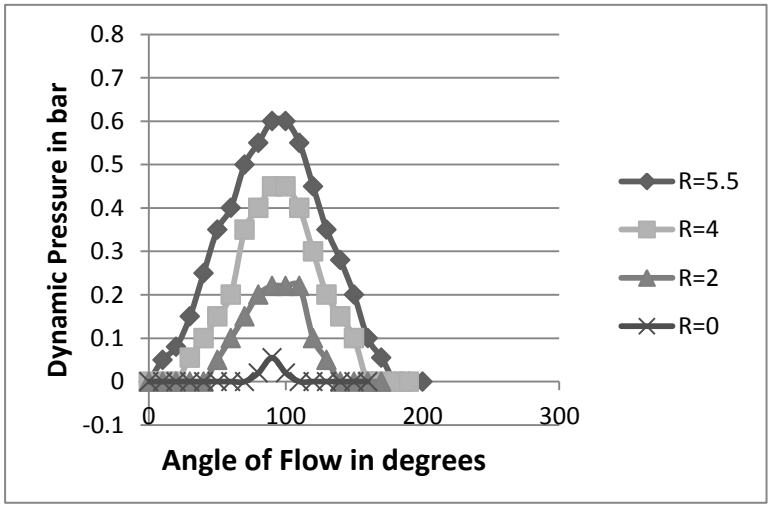

Figure 33 : Dynamic Pressure vs Angle of Flow for Hole 2

- Hole 3 (50 mm from inlet)

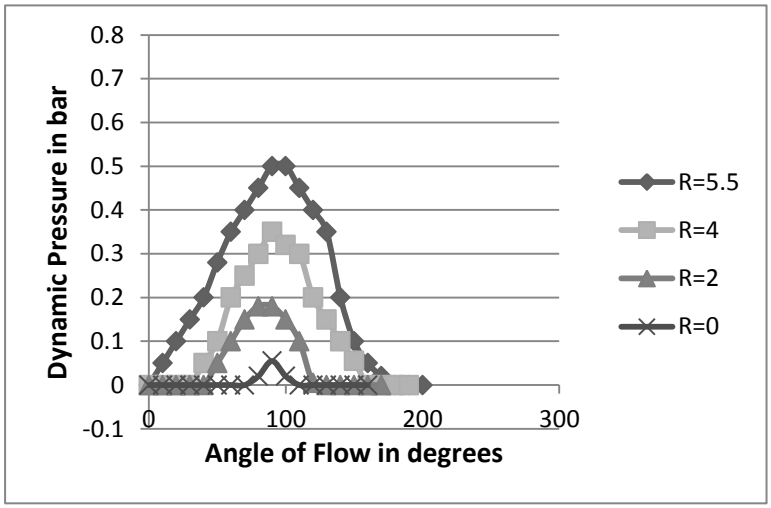

Figure 34 : Dynamic Pressure vs Angle of Flow for Hole 3

- Hole 4 (70 mm from inlet)

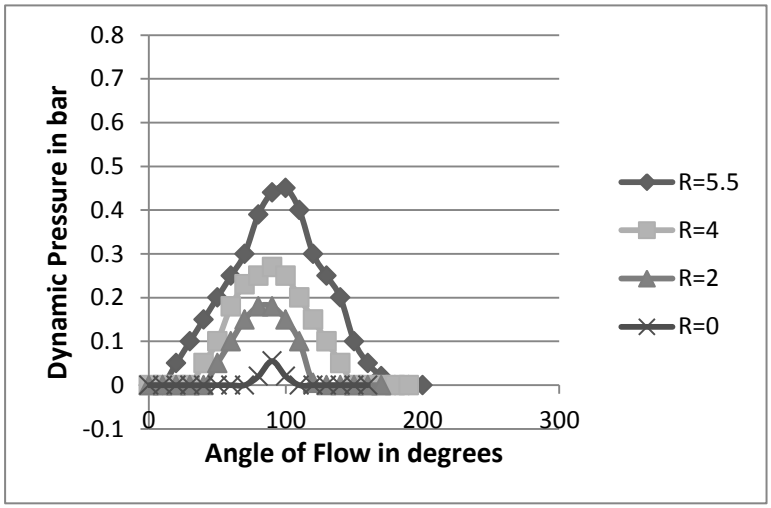

Figure 35 : Dynamic Pressure vs Angle of Flow for Hole 4

- **Inlet Pressure - 4bar**

  - Hole 1 (10 mm form inlet)

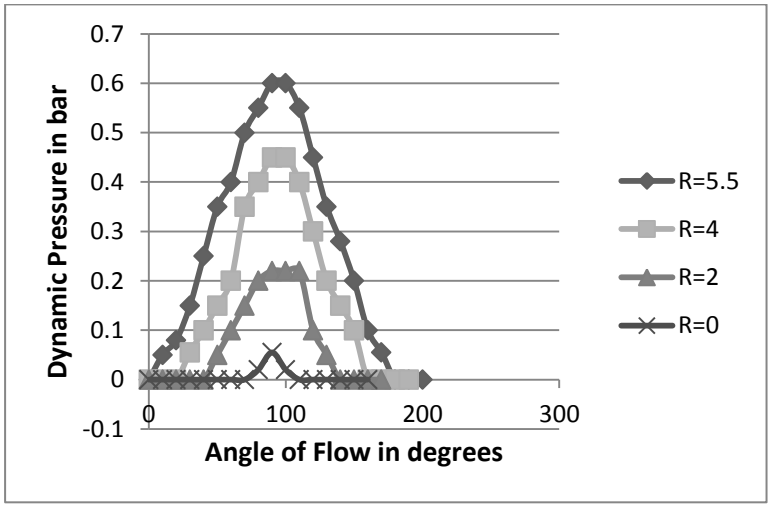

Figure 36 : Dynamic Pressure vs Angle of Flow for Hole 1

  - Hole 2 (30 mm from inlet)

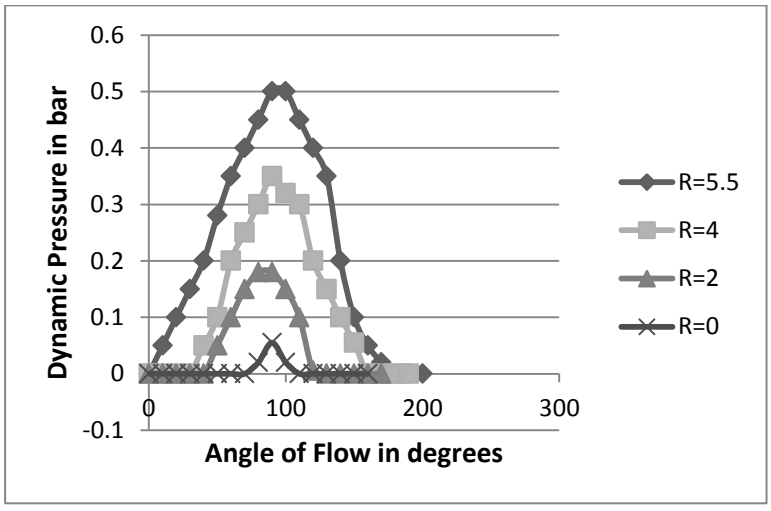

Figure 37 : Dynamic Pressure vs Angle of Flow for Hole 2

- Hole 3 (50 mm from inlet)

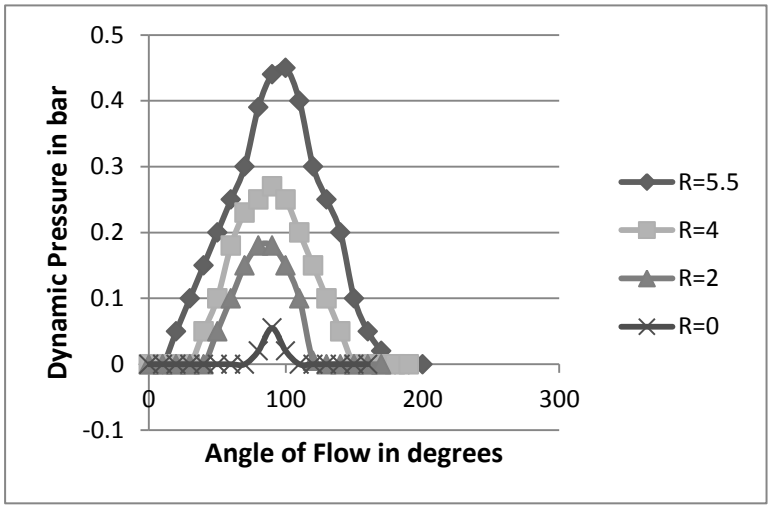

Figure 38 : Dynamic Pressure vs Angle of Flow for Hole 3

- Hole 4 (70 mm from inlet)

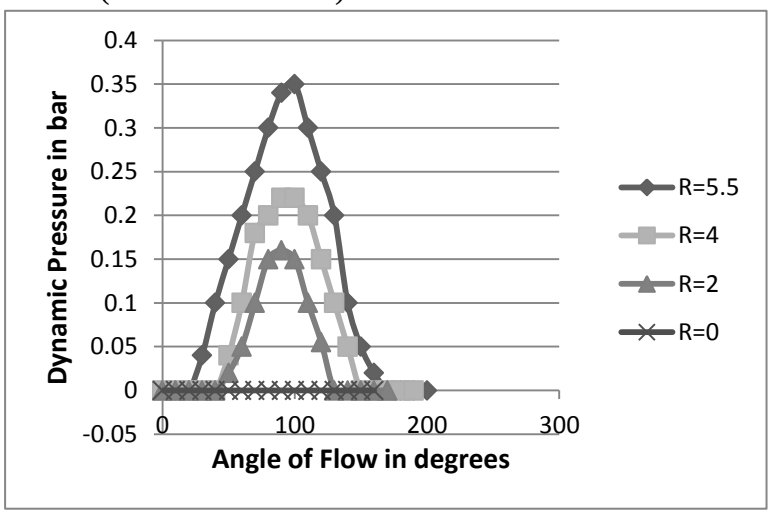

Figure 39 : Dynamic Pressure vs Angle of Flow for Hole 4

Results

The dynamic pressure indicates the direction of flow of the vortex. The intensity indicated the difference in velocities. The velocity was highest at the periphery and went on decreasing towards the centre.

As the vortex advanced along the length of the tube its velocity went on decreasing. At a certain point before the obstruction the flow reaches complete stagnation before reversing.

Comparison with Previous Documented Results

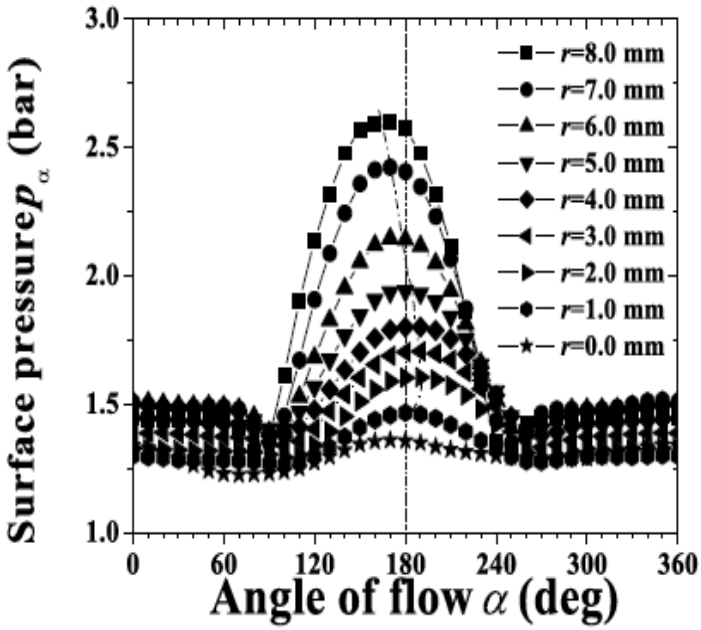

Figure 40 : Surface pressure gradients by C. Gao

The figure above indicates absolute dynamic pressure with respect to angle of flow whereas the one below shows gauge pressure. In the performed analysis the marking of angles had a shift of 90 degrees with respect to the previous observation. The pattern of the observations remains the same.

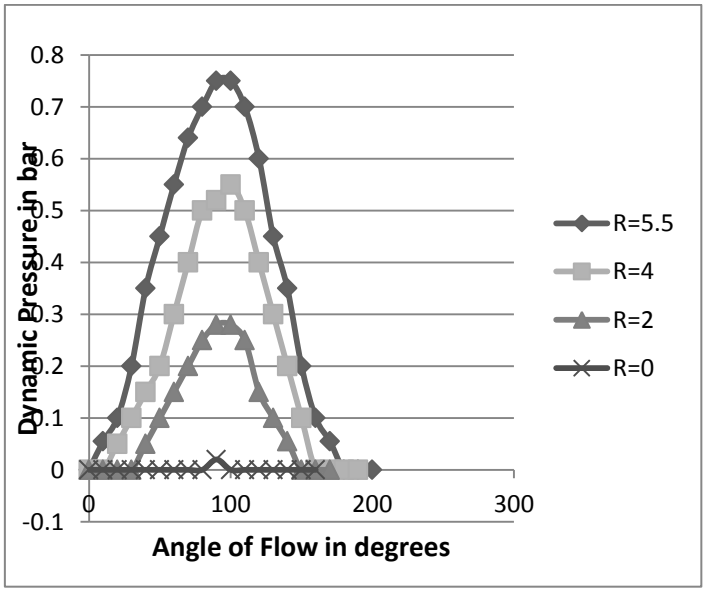

Figure 41 : Dynamic Pressure gradients for current analysis

Chapter 7 : Thermodynamic Analysis

The performance of a vortex tube must be compared to the conventional refrigeration cycles. To obtain the parameters for comparison thermodynamic analysis must be done.

Parameters for thermodynamic analysis

1. Cold Mass Fraction
   The cold mass fraction is the ratio of mass of cold air that is released through the cold end of the tube to the total mass of the input compressed air. It is represented as follows
   ε = mc/mi = (Ti-Th)/ (Tc-Th)

2. Cold temperature drop
   Cold air temperature difference or temperature reduction is defined as the difference between inlet flow temperature and cold air temperature:
   $\Delta T\ c = Ti - Tc$

3. Hot Temperature difference
   Similarly, hot air temperature difference is defined as
   ΔTh = Th – Ti

4. Refrigerating Effect
   The refrigerating /cooling effect produced by the cold air of vortex tube is give as
   $Qc = mc\ Cp\ (Tc - Ti)$

5. Heating Effect
   Since cooling and heating streams are obtained simultaneously the heating effect produced by the vortex tube is give as
   Qh = mh Cp (Th – Ti)

6. Coefficient Of Performance
   COP provides a strong basis for comparing refrigeration systems.

$$COP_{ref} = \frac{\gamma\varepsilon}{\gamma - 1}\ \frac{(T_i - T_c)}{T_i ln\left(\frac{p_i}{p_a}\right)}$$

$$COP_{heat\ pump} = \frac{\gamma(1-\varepsilon)}{\gamma - 1}\ \frac{(T_h - T_i)}{T_i ln\left(\frac{p_i}{p_a}\right)}$$

Therefore , we will be using above formulae for our further calculations. The relations have been predefined by Ahlborn, Gupta. U, thermodynamic analysis.

First let us establish the inlet air conditions. Temperature of air is assumed to be constant at 298 K. The pressure and flow rate are controlled by simple throttling. Following is the relation between the pressure and flow rate.

Table 8 : Inlet Pressure vs Flow rate

Pressure	Volume Flow Rate in LPM	Mass Flow Rate kg/s
6.2	116	0.0163
5.5	108	0.0152
5	100	0.01411
4.5	95	0.0134
4	88	0.01242
3.5	80	0.01129
3	75	0.0105
2.5	65	0.009177
2	56	0.0079

The analysis is done at the pressure of 6.2 bar. Therefore mi = 0.0163 kg/s

Thermodynamic analysis for Cone Geometry (since it offered better flow rates)

Table 9 : Thermodynamic Analysis - Calculations

Cold Temperature (K)	Cold Flow rate (kg/s)	Cold fraction	Refrigerting Effect (Watts)	COP refrigeration
253	0.0013	0.08	58.79	0.24
256	0.001546	0.095	65.256	0.227
260	0.00165	0.101	63.015	0.204
263	0.0017	0.104	59.79	0.187
265	0.00189	0.115	62.68	0.174
267	0.002213	0.1357	68.94	0.16
270	0.002408	0.147	67.76	0.1429
273	0.002706	0.166	68	0.124

The refrigerating effect is higher at higher flow rates. Therefore when a minimum temperature is not the requirement, higher flow rates can be used for better cooling. For minimum temperatures, flow rate must be compromised.

Chapter 8 : Conclusions

Above experiment and analysis was carried out to achieve the following two objectives.

1. To recreate and verify the analysis which is presented in previous papers.
2. To optimize the performance of the vortex tube by varying the geometrical parameters (in this case the hot exit geometry).

The above objectives were achieved successfully and following conclusions can be made

1. CFD analysis provided near accurate results in all cases. This validates the use of CFD for analysis of vortex tube.
2. The temperature drop of the vortex tube, in a general case, can be varied by varying the back pressure at the hot end.
3. The geometry of the obstruction does affect the performance of the vortex tube to a certain extent.
4. Protrusion in the geometry can improve the flow rate for the same minimum temperature and orifice area.
5. For better flow rates we need to compromise on minimum temperature
6. Better cold flow heat drop is attained at higher flow rates, and thus must be preferred for spot cooling applications.
7. Coefficient of Performance (refrigeration) of a vortex tube is very low (<1). Therefore, it cannot replace traditional refrigeration techniques in general applications.

Chapter 9 : Future Scope

The basic aim of this project was to observe the working of vortex tube and study the parameters affecting it. One of the factors was focussed upon in this research. However the vortex tube can be optimized by various other methods.

1. Control Valves at Hot End
   Analysis can be done on the performance of vortex tube using commercial control valves for the hot end. Comparison can be done for the most optimum valve which can be used in this case.
2. Calculation of Coolant Savings
   The amount of coolant that can be saved can be analysed. Optimum flow rate combination of cool air and liquid coolant must be determined.
3. Heat Load Calculations
   Use of vortex tube as a cabinet cooler requires heat load analysis
4. Instrumentation
   Devices can be used to indicated temperature depending upon the control valve positions. Proper calibration is required in this case.

References

1. U. Behera, P.J. Paul, S. Kasthurirengan, R. Karunanithi, S.N. Ram, K. Dinesh, S. Jacob, CFD analysis and experimental investigations towards optimizing the parameters of Ranque–Hilsch vortex tube
2. B. Ahlborn, J.U. Keller, R. Staudt, G. Treitz, E. Rebhan, Limits of temperature separation in a vortex tube.
3. N. Pourmahmoud, A. Hassan Zadeh, O. Moutaby, A. Bramo, Computational Fluid Dynamics Analysis Of Helical Nozzles Effects On The Energy Separation In A Vortex Tube, Thermal Science, Year 2012, Vol. 16, No. 1, pp. 151-166
4. A. Bramo And N. Pourmahmoud, Computational Fluid Dynamics Simulation Of Length To Diameter Ratio Effects On The Energy Separation In A Vortex Tube, Thermal Science, Year 2011, Vol. 15, No. 3, pp. 833-848
5. Prabakaran.J, Vaidyanathan.S, Effect Of Diameter Of Orifice And Nozzle On The Performance Of Counter Flow Vortex Tube, International Journal of Engineering Science and Technology Vol. 2(4), 2010, 704-707
6. H.M. Skye, G.F. Nellis, S.A. Klein, Comparison of CFD analysis to empirical data in a commercial vortex tube, International Journal of Refrigeration 29 (2006) 71–80
7. U. S. Gupta, M. K. Joshi, Saurabh Rai, Thermodynamic Analysis Of Counter Flow Vortex Tube, International Journal of Engineering Research & Technology (IJERT) Vol. 2 Issue 2, February- 2013
8. Ronán Oliver, Fergal Boyle, Anthony Reynolds, Computer Aided Study of the Ranque–Hilsch Vortex Tube Using Advanced Three-Dimensional Computational Fluid Dynamics Software, Proceedings of the 6th WSEAS International Conference on Applied Computer Science, Tenerife, Canary Islands, Spain, December 16-18, 2006, Page 478
9. C. Gao, Experimental Study On the Ranque-Hilsch Vortex Tube
10. Anayet U. Patwari, N.M Reehan, Adib Bin Rashid and Ashikur Rahman, Computational Analysis Of The Effect Of Vortex Parameters In A Vortex Tube
11. N. Pourmahmoud, Alireza Izadi, Amir Hassanzadeh, Ashkan Jahangiramini, Computational Fluid Dynamics Analysis Of The Influence Of Injection Nozzle Lateral Outflow On The Performance Of Ranque-Hilsch Vortex Tube

Images

Figure 42 : Assembly of Vortex Tube

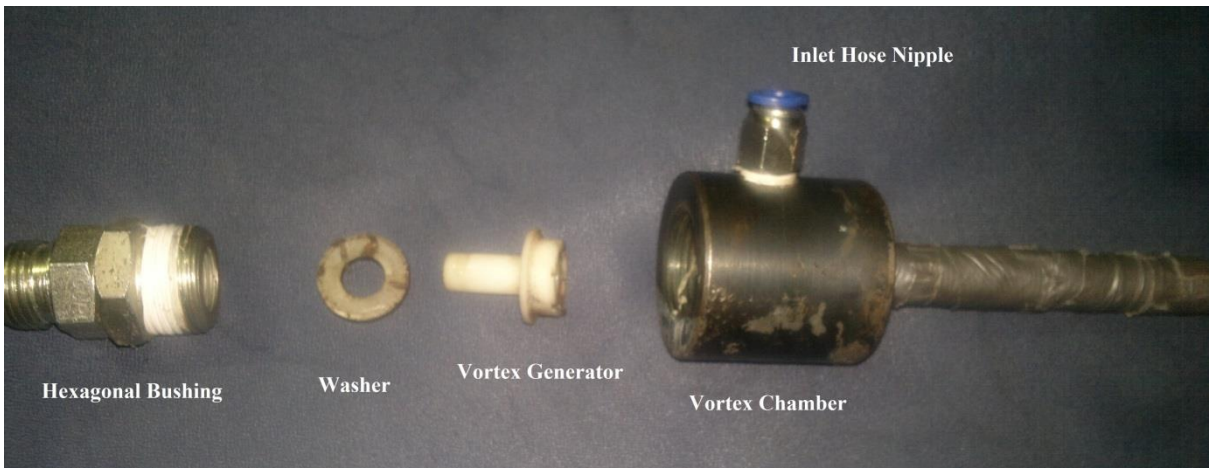

Figure 43 : Exploded View of Vortex Tube

Part Descriptions

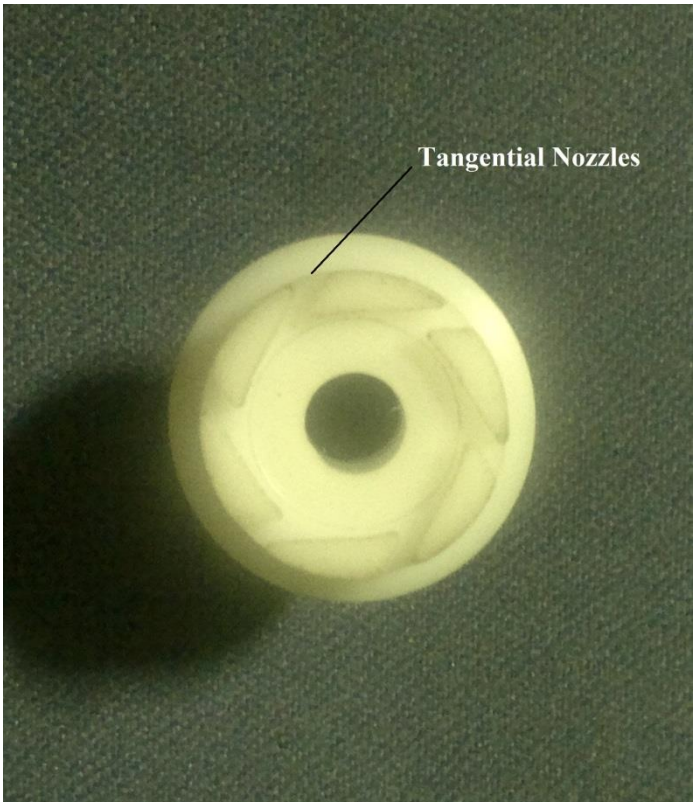

Figure 44 : Vortex Generator

Fig. 45 Hexagonal Bushing

(1/2 bsp x 3/8 bsp)

Fig. 46 Hose Nipple (8mm, ¼ bsp)

Vortex Chamber

½ bsp threading

Inlet Nozzle 3 mm diameter

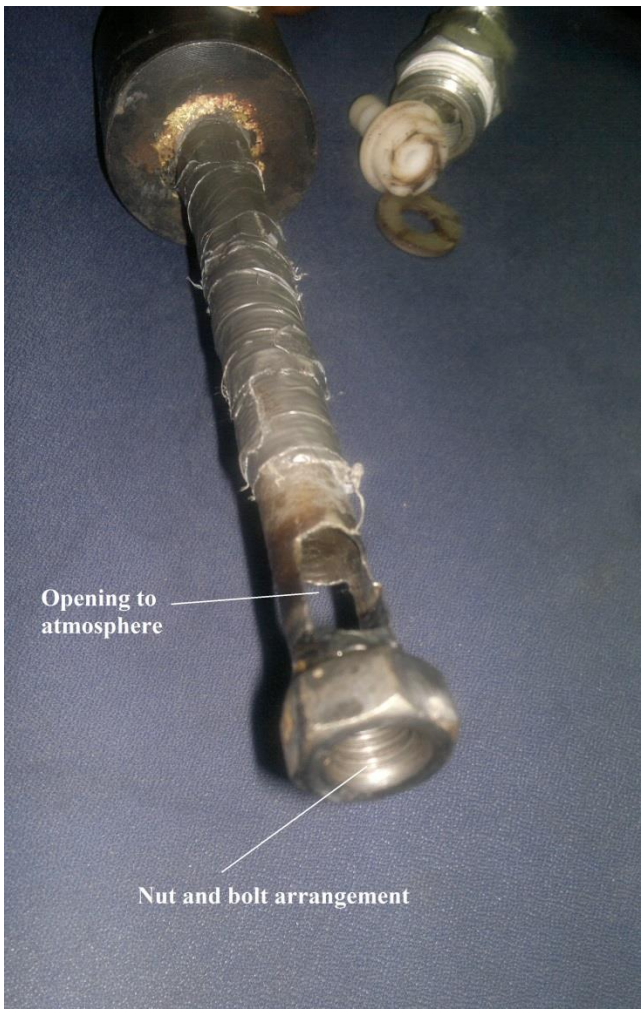

Hot End Arrangement